Accepted Manuscript

Petroleum Geoscience

New Insights into the Structure, Geology and Hydrocarbon Prospectivity along the Central-Northern Corona Ridge, Faroe-Shetland Basin

Lucinda K. Layfield, Nick Schofield, David W. Jolley, Simon P. Holford, Tudor-Remus Volintir, Ben A. Kilhams, David K. Muirhead & Helen Cromie

DOI: https://doi.org/10.1144/petgeo2021-090

To access the most recent version of this article, please click the DOI URL in the line above. When citing this article please include the above DOI.

Received 4 November 2021
Revised 6 June 2022
Accepted 14 July 2022

New Insights into the Structure, Geology and Hydrocarbon Prospectivity along the Central-Northern Corona Ridge, Faroe-Shetland Basin

Lucinda K. Layfield[1]*, Nick Schofield[1], David W. Jolley[1], Simon P. Holford[2], Tudor-Remus Volintir[3], Ben A. Kilhams[1], David K. Muirhead[1], Helen Cromie[4]

[1]*Department of Geology and Geophysics, University of Aberdeen, King's College, Aberdeen, AB24 3EU, UK.*

[2]*Australian School of Petroleum and Energy Resources, University of Adelaide, Adelaide, SA, Australia.*

[3]*Schlumberger, Bd. Timișoara 15, București 061344, Romania.*

[4]*TotalEnergies Upstream Danmark A/S, Amerika Plads 29, 2100 Copenhagen, Denmark.*

LKL, 0000-0002-5693-4959, DWJ, 0000-0003-0909-2952, SPH, 0000-0002-4524-8822, BK, 0000-0002-4444-6800, DM, 0000-0003-2065-6042.

**Correspondence (e-mail: l.layfield.18@abdn.ac.uk)*

Present address: HC, Ørsted Wind Power, Nesa Allé 1, 2820 Gentofte, Denmark.

Abstract: The Faroe-Shetland Basin (FSB) is one of the only significant exploration frontiers remaining on the UK Continental Shelf. Over half of the basin's discovered reserves and resources lie along two intra-basinal highs, the Corona Ridge and Rona Ridge. In contrast to the Rona Ridge, the central-northern Corona Ridge has received much less attention. To reveal new insights into the geology, structural configuration, and hydrocarbon prospectivity of the central-northern Corona Ridge we analyse 3D seismic data and data from exploration wells 213/23-1 (Eriboll), 214/21a-2 (South Uist) and 213/25c-1V (North Uist). This study extends the Colsay T40-T45 sub- and intra-basaltic play concept from the Rosebank Field NE along the Corona Ridge, at least into 213/23-1. Analysis also suggests that no Triassic strata are present within 213/23-1, challenging the previous understanding of Triassic distribution within the central FSB. Our findings show that the central-northern Corona Ridge is structurally complex, comprised of a series of discrete basement bounding faults, down-flank fault terraces and faults which are oblique to the dominant NE-SW-striking structural fabrics of the FSB.

The Faroe-Shetland Basin (FSB), located west of the Shetland Isles on the NE Atlantic continental margin (Fig. 1), is one of the only remaining significant exploration frontiers on the UK Continental Shelf (UKCS) and will also arguably be one of the most important areas to contribute to indigenous oil and gas supply in the next 40 years (Austin *et al.* 2014; Ellis & Stoker 2014). As of September 2021, the region is estimated to hold *c.* 3.7 billion barrels oil equivalent (BBOE) of discovered reserves and contingent resources, around 30% of the UK's total (2P and 2C; NSTA 2019). In 2019, the UKs North Sea Transition Authority (NSTA) estimated mean yet-to-find resources of 5.8 BBOE within the West of Shetland region, totalling 38% of estimated yet-to-find resources across the entire UKCS (encompassing lead, prospect, and play-level prospective resources; NSTA 2019).

Particularly prospective areas of the FSB include intra-basinal highs; in total, over half of the discovered reserves and contingent resources in the basin are situated on the Corona and Rona Ridge (Fig. 1) (Austin *et al.* 2014; Scotchman *et al.* 2016; NSTA 2019). Significant discoveries, some now developed and in production, have been made along the Rona Ridge (Fig. 1b) within early Cretaceous shallow to marginal marine (Victory Field; Goodchild *et al.* 1999) and marine (Edradour Field; Clark *et al.* 2020) sandstones, fractured Precambrian crystalline basement rocks (e.g., Clair Ridge; Robertson *et al.* 2020) and Devonian-age siliciclastic rocks of the Lower Clair Group (Clair Field, Robertson *et al.* 2020) (Fig. 2).

Exploration focused along the Corona Ridge has provided encouraging results (e.g., Rosebank and Cambo Fields, Lochnagar and Blackrock discoveries, Fig. 1b). However, in contrast to the Rona Ridge (on which the Clair and Lancaster Fields are developed), as of June 2022, none of the discoveries made along the Corona Ridge have been sanctioned for development. The 300 million barrels of oil equivalent (mmboe) (recoverable) Rosebank Field, reservoired within the upper Paleocene–lower Eocene-aged fluvial-deltaic intra- and sub-basaltic Colsay Member (T40-T45) sandstone units, is currently awaiting a final investment decision (FID, estimated in 2022), 18 years since its discovery in 2004 (Siccar Point Energy 2020a). Planned sanction of the Cambo Field (30 km SW of Rosebank) was expected within 2022 with first oil projected for 2025, 23 years after the discovery of 800 mmboe (in place) within Hildasay Member (T45) sandstones in 2002 (Siccar Point Energy 2020a, 2020b).

The Cambo and Rosebank discoveries currently represent the largest undeveloped accumulation in the UKCS (as of June 2022), totalling *c.* 700 mmboe of recoverable resources (Austin *et al.* 2014; Siccar Point Energy 2020a). In addition to Cambo and Rosebank, hydrocarbon shows, and discoveries have been encountered within multiple stratigraphic intervals along the Corona Ridge, including the Carboniferous North Uist (213/25c-1V), Jurassic Lochnagar (213/27-1Z), Paleocene Bunnehaven (214/09-1), Paleocene–Eocene Blackrock (204/05b-2) and Eocene Tobermory (214/04-1) discoveries (Figs 1 & 2).

Whilst hydrocarbon shows and discoveries prove a working petroleum system is present both along the Corona Ridge and within the basins bound by the Corona Ridge, as highlighted by Scotchman *et al.* (2006, 2016), Mark *et al.* (2018a, 2018b) and Gardiner *et al.* (2019), many aspects of the region's petroleum geology are still not fully understood – emphasised by recent (2019) disappointing results of wells drilled along the Corona Ridge (Lochnagar appraisal, well 213/27-3Z, Fig. 1b) and *c.* 15 km from the northern Corona Ridge (Lyon prospect, well 208/02-1, Fig. 1b; *see* P1854 Relinquishment Report 2020).

Within the last two decades, exploration focus and success along the Corona Ridge has largely been confined to the post-rift Paleocene–Eocene-aged reservoirs around the Rosebank Field, located along the southern part of the Corona Ridge (Smallwood & Kirk 2005; Loizou 2014). Consequently, published literature of the structure, evolution and geology of the central-northern Corona Ridge is sparse, especially when compared with the prolific Rona Ridge. This is largely the result of basaltic lava cover which extends from the Faroe Islands into the FSB over much of the Corona Ridge, resulting in challenging sub-basaltic seismic imaging (Schofield & Jolley 2013). Published research has largely overlooked the possible distribution of intra- and sub-basaltic Paleocene–Eocene-aged (sequence T40-T45) reservoirs NE of the Rosebank Field and older pre-rift (Devonian–Jurassic) strata present along the central-northern Corona Ridge. Many of the exploration wells drilled along the Corona Ridge were drilled within the late 1990s and early 2000s (e.g., 213/23-1, 214/04-1 and 214/09-1, Fig. 1b), prior to key advancements in the understanding of the evolution and lithostratigraphy of the FSB and specifically the Corona Ridge.

At the time of publication, over 100 mmboe of condensate and 656 billion cubic feet (bcf) of stranded gas lies undeveloped along the central-northern Corona Ridge, currently viewed as uneconomic for development without a substantial discovery nearby to warrant the development of gas infrastructure as a tieback option (P50 post-drill in place volume estimates; Tobermory 464 bcf, 214/04-1 Post-Drill Report 2000; Bunnehaven 192 bcf, 214/09-1 Post-Drill Well Summary Report 2001; North Uist 104 mmboe, P.1192 Relinquishment Report 2017).

The objective of this paper is to provide new insights into the structural configuration, geology, and hydrocarbon prospectivity of the central-northern Corona Ridge, which lies within an area in need of a substantial discovery, through the interpretation of 3D seismic data integrated with post-well analysis of three exploration wells (213/23-1 (Eriboll), 214/21a-2 (South Uist) and 213/25c-1V (North Uist), Fig. 1b).

By analysing well data, we interpret that no Triassic-age strata are present within 213/23-1 (Eriboll) and possibly the central FSB entirely, challenging the previous understanding of the distribution of Triassic strata within the centre of the basin (Quinn & Ziska 2011; Stoker *et al.* 2014; Stoker *et al.* 2017b). We also extend the Colsay Member intra- and sub-basaltic play concept NE along the Corona Ridge from the Rosebank Field into 213/23-1 (Eriboll). Our findings also suggest that the central-northern Corona Ridge is structurally complex with evidence of N-S and NNW-SSE-striking normal faults which are oblique to the basinal NE-SW-striking structural trends.

Geological History

The Faroe-Shetland Basin (FSB) is located between the Shetland and Faroe Islands on the NE Atlantic passive continental margin of NW Europe (Fig. 1), bound by the Wyville-Thomson Ridge (UKCS) to the SW and the Møre Marginal High (Norwegian Continental Shelf) to the NE (Ziska & Varming 2008; Ritchie *et al.* 2011). The FSB is up to 400 km long and 250 km wide and is constituted from a series of smaller rift-related sub-basins which formed throughout several main phases of extension between the early Cretaceous and early Cenozoic (Ritchie *et al.* 2011). Sub-basins are separated by NE-SW-trending, intra-basinal structural highs comprising Precambrian crystalline rock (Figs 1 & 3) which are commonly unconformably capped by incomplete occurrences of pre-rift Paleozoic to Jurassic sedimentary rocks (Lamers & Carmichael 1999; Sørensen 2003; Peacock & Banks 2020).

Precambrian crystalline basement, observed onshore Scotland as the Lewisian Gneiss Complex, is understood to have formed after Neoarchean pluton emplacement and cooling between 2700-2800 Ma (Bonter & Trice 2019; Holdsworth *et al.* 2019; Peacock & Banks 2020). Offshore

within the FSB, basement rocks are generally considered to be equivalent to the Lewisian Gneiss Complex (Holdsworth *et al.* 2019) and have been cored and dated to the Neorchean (Ritchie *et al.* 2011). Wells which have penetrated crystalline basement within the FSB have typically encountered Neoarchean quartzofeldspathic granodioritic orthogneisses (Gardiner *et al.* 2019; Holdsworth *et al.* 2019). Towards the north of the FSB, on the West Shetland and North Shetland Platforms, the nature of the basement rock changes from crystalline to Neoproterozoic Moine and Dalradian rocks and Paleozoic Caledonian rocks (Kinny *et al.* 2005; Ritchie *et al.* 2011; Holdsworth *et al.* 2019).

Since Neoarchean pluton emplacement, crystalline basement has been subject to the complex structural evolution of the FSB. Prominent NE-SW-striking structural trends present throughout the FSB are thought to be inherited from pre-existing structural fabrics within basement rocks. Structural fabrics are thought to have initially developed as Precambrian shear zones during the Archaean and Proterozoic which were later reactivated as both thrusts and deep-rooted strike-slip faults during the Cambrian–Devonian Caledonian Orogeny (Coward 1990; Doré *et al.* 1997). During Devonian orogenic collapse strike-slip faults were then reactivated as normal faults (Moy & Imber 2009; Ritchie *et al.* 2011).

The predominant NE-SW-striking structural fabric has since been periodically exploited during multiple phases of crustal extension from the Permo-Triassic to the early Cenozoic (UK Atlantic Margin events, Fig. 2), separating the once contiguous crystalline basement into a series of intra-basinal highs (Figs 1a & 3) (Doré *et al.* 1997, 1999; Ritchie *et al.* 2011; Ellis & Stoker 2014; Schofield *et al.* 2020).

The initial phases of sedimentary input within the FSB are attributed to the erosion of Caledonian topography into post-orogenic Devonian–Carboniferous intermontane basins, thought to be generated by extensional collapse of the Caledonian fold-and-thrust belt (Underhill 2003; Ritchie *et al.* 2011; Smith & Ziska 2011; Ellis & Stoker 2014; Stoker 2016). Devonian to Carboniferous-age basins (e.g., the Clair Basin on the Rona Ridge; Nichols *et al.* 2005) accommodated the deposition of the Clair Group, dominated by fluvial sequences with lacustrine and aeolian influence (Underhill 2003; Smith & Ziska 2011). These deposits rest unconformably on

Precambrian basement rock and form the main reservoir sequences of the Clair Field (Ogilvie *et al.* 2015; Robertson *et al.* 2020). Where penetrated by wells within the FSB on the Rona Ridge, the proven thickness of the Clair Group varies from absent (e.g., 205/21-1A and 206/12-1, Fig. 1b) to *c.* 1000 m thick (Ziska & Anderson 2005), reflecting a varied history of deposition and post-depositional erosion. Subsequent basin development of the FSB, after the Devonian–Carboniferous, primarily relates to the Atlantic rift system active throughout the Triassic to Cretaceous, contributing to the fragmentation of Pangaea and the opening of the Atlantic (Roberts *et al.* 1999; Ellis & Stoker 2014; Stoker 2016; Stoker *et al.* 2017b).

Initial rifting is indicated by large thicknesses of Permian–Triassic strata deposited within the West Orkney and Papa Basins (e.g., 2436 m in 205/27a-1, Fig. 1b; Ritchie *et al.* 2011) and inferred from seismic profiles (Quinn & Ziska 2011; Stoker *et al.* 2017b). Permo-Triassic extension is thought to be concentrated within the Papa, West Shetland, West Orkney and Unst basins (Fig. 1) where Permian strata are proven (e.g., 205/27a-1). This early rifting event is thought to have exploited existing basement structural fabrics, leading to the formation of NE-SW-trending half-graben basins filled with aeolian, fluviatile and lacustrine sequences, though differentiation of Permian–Triassic sequences is often challenging due to the lack of diagnostic biostratigraphy (Swiecicki *et al.* 1995; Štolfova & Shannon 2009; Ritchie *et al.* 2011; Stoker *et al.* 2017b). The presence of Permian–Triassic strata within the FSB is mostly interpreted to be concentrated around the present-day margins of the basin (e.g., 204/19-1, 204-19-9 and 204/29-1, Fig. 1b), with the exception of 213/23-1 (Eriboll) and 214/09-1 (Bunnehaven) which are located within the central FSB along the Corona Ridge (Quinn & Ziska 2011). Semi-arid fluvial-lacustrine conditions prevailing throughout the Triassic are expressed within the FSB as variable thicknesses of the Papa Group ranging from 426 m within the Judd sub-basin (204/29-1, Fig. 1b) to 73 m interpreted on the Corona Ridge by Quinn & Ziska (2011) (73 m 'indeterminate' section in 214/09-1, Bunnehaven; 214/09-1 Post-Drill Well Summary 2001).

Post-rift thermal subsidence coupled with global sea level rise initiated a marine incursion during the early Jurassic, leading to the deposition of the shallow marine Skerry Group sequences, although well penetrations of Lower Jurassic strata are sparse within the FSB (Dean *et al.* 1999;

Ritchie & Varming 2011). Thermal subsidence continued until the middle to late Jurassic, when renewed extension of existing Permo-Triassic half-grabens occurred, thought to be related to synchronous rifting in the North Sea (Ritchie *et al.* 2011). Numerous wells, largely confined to intra-basinal highs including the Corona Ridge, have penetrated the Kimmeridge Formation comprising the sand-rich Rona Sandstone Member and organic-rich Kimmeridge Clay Member of the Humber Group (mean total organic content of *c.* 4.5% for FSB wells; Scotchman *et al.* 1998), deposited throughout pre-dominantly marine conditions (Ritchie & Varming 2011). The majority of the discoveries made along the Corona Ridge are thought to be sourced from the organic-rich Kimmeridge Clay (Scotchman *et al.* 2016; Gardiner *et al.* 2019).

The present-day geometry of the FSB, along with the adjacent Rockall and Møre basins, was mainly developed by widespread extension initiated within the early Cretaceous, which is largely responsible for the present-day structures of the Corona Ridge (Ritchie *et al.* 2011; Hardman *et al.* 2018). Extension along the NE Atlantic Margin during the Cretaceous was concurrent with northward propagation of the Central Atlantic rift system, which became relatively inactive after the late Cretaceous period (Doré *et al.* 1999; Fletcher *et al.* 2013; Stoker 2016; Schofield *et al.* 2020). Deposition of thick (up to 5 km) deep marine Cretaceous successions occurred on the hanging walls of major fault systems (Larsen *et al.* 2010; Stoker 2016; Gardiner *et al.* 2019).

Post-rift thermal subsidence was terminated by a rifting phase during the early Paleocene (concentrated 400 km to the west) which exploited the established Mesozoic normal rift system and occasionally manifests on the Corona Ridge as minor normal faulting on reactivated major bounding faults only (Doré *et al.* 1999; Smallwood & Gill 2002; Ellis & Stoker 2014). The NE Atlantic Margin experienced significant igneous activity during the Paleocene to Eocene, prior to (*c.* 62-58.5 Ma) and during (*c.* 57-54 Ma) continental break up between Greenland and NW Europe (Watson *et al.* 2017; Jolley *et al.* 2021).

This study employs the British Geological Survey (BGS) lithostratigraphy from Ritchie *et al.* (2011), which adopts the BP Paleocene T-sequence framework of Ebdon *et al.* (1995) (Fig. 4) for consistency with previous studies. The regional onset of volcanism within the FSB occurred prior to

continental breakup and is recorded by Danian (66-61.6 Ma) to Selandian-age (61.6-59.2 Ma) basaltic tuffs of sequences T10-T36 (Watson *et al.* 2017; Jolley *et al.* 2021). Marine conditions prevailed throughout the Paleocene, accompanied by the deposition of a series of major turbidite fans in adjacent basins (e.g., the Flett, Judd and Nuevo sub-basins) during the mid-Paleocene (sequence T31-T36) (Stoker & Varming 2011).

Rifting was followed by uplift that began during the late Paleocene (Ebdon *et al.* 1995). Subsequent emergence of areas adjacent to the FSB (e.g., the East and West Shetland Platforms) facilitated the deposition of Thanetian (59.2-56 Ma) to Ypresian-age (56-47.8 Ma) major prograding shelf-margin systems (sequences T38-T40) during the late Paleocene–early Eocene (Stoker & Varming 2011).

The main phase of extrusive volcanism occurred within the early Eocene during continental break up, with the eruption of a widespread extrusive basaltic component comprised predominantly of thick flood basalt (lava) sequences of the Faroe Islands Basalt Group (FIBG) (Bell & Jolley 1997; Passey & Hitchen 2011; Schofield *et al.* 2017; Jolley *et al.* 2021). Flood basalt eruption during the deposition of Colsay Member sandstone units (sequence T40-T45) led to the formation of intra-basaltic plays of the Rosebank Field along the Corona Ridge (Jolley & Bell 2002; Passey & Jolley 2009; Schofield & Jolley 2013; Hardman *et al.* 2018). The emplacement of an extensive suite of mafic intrusions, the Faroe Shetland Sill Complex (FSSC), occurred before and during continental breakup between *c.* 58-55 Ma (Schofield *et al.* 2017; Watson *et al.* 2017; Jolley *et al.* 2021).

A migration of the Central Atlantic rift system extension locus to the west of the present-day Faroes occurred during the early Eocene, synchronous with the onset of North Atlantic seafloor spreading between *c.* 56-55 Ma (Ellis & Stoker 2014; Stoker *et al.* 2017a, 2017b; Jolley *et al.* 2021). Supra-basaltic Hildasay Member (sequence T45) sandstones of the Flett Formation are overlain by the Balder Formation (sequence T50) which acts as a regional seismic marker (Ebdon *et al.* 1995; Watson *et al.* 2017). A return to deep marine conditions in the early Eocene resulted in the deposition of the Stronsay Group (sequence T60-T98; Stoker *et al.* 2012) which contains a number of submarine fan complexes, including the mid-Eocene Breydon, Caledonia, Rothbury, and Strachan

Fans which have proven sandstone-rich along the Corona Ridge, with the latter a reservoir for the Tobermory gas field (Mobil North Sea Limited 1999a, 1999b; Smallwood & Gill 2002; Stoker & Varming 2011).

The FSB was subject to multiple further episodes of tectonism during the late Paleocene, early to mid-Eocene and Oligo-Miocene (Smallwood & Maresh 2002; Smallwood 2004; Ellis *et al.* 2009). Throughout this time, inversion along intra-basinal highs facilitated the growth of elongate anticlines and domal structures with four-way closures within Cretaceous to Cenozoic-age strata (Sørensen 2003; Doré *et al.* 2008; Ritchie *et al.* 2008). This inversion was also most likely responsible for many of the traps present along the Corona Ridge but is also considered to be responsible for the breach of pre-existing top seals and subsequent leakage (Ritchie *et al.* 2011; Ellis & Stoker 2014; Stoker *et al.* 2017a).

Previous structural interpretation of the Corona Ridge

The most prominent structural elements in the FSB are the NE-SW-trending intra-basinal highs composed of Precambrian crystalline basement, including the Corona Ridge (and other structural highs such as the Rona Ridge). In this study we follow the definition of basement high proposed by Peacock & Banks (2020, p. 18), 'an area in which the basement rocks [Precambrian crystalline rocks] are significantly higher than in the surrounding areas'. Within the Peacock & Banks (2020) definition, the word significantly is used in the context of influencing the petroleum system, e.g., source rock maturation and subsequent migration. The term central-northern Corona Ridge is used herein to refer solely to the Precambrian crystalline rocks which form the intra-basinal high itself.

Rumph *et al.* (1993) introduced the term Corona Ridge, although the ridge was previously variably referred to as the Mid-Faeroe Ridge (Mudge & Rashid 1987; BGS 1996; Hughes *et al.* 1997), Central High Complex (Hitchen & Ritchie 1987), Axial Opaque Zone (Ridd 1981, 1983) and North Westray Ridge (Iliffe *et al.* 1999). Early conceptual models for the development of the Corona Ridge include a Cenozoic igneous complex similar to the Wyville-Thompson Ridge (Ridd 1981; Hitchen &

Ritchie 1987) or, as the Corona Ridge is now known, a Lewisian-age crystalline basement-cored structural high analogous to the Rona Ridge (Mudge & Rashid 1987).

Numerous authors extend the ridge SW to the Cambo High (Ellis *et al.* 2009; Ritchie *et al.* 2011; Hardman *et al.* 2018) and NE towards the quadrant 217 (Mudge & Rashid 1987; BGS 1996; Hughes *et al.* 1997; Dean *et al.* 1999; Ellis *et al.* 2009; Ritchie *et al.* 2011). The complexity of the Corona Ridge varies between publications. Many publications (Mudge & Rashid 1987; Rumph *et al.* 1993; Ebdon *et al.* 1995; BGS 1996; Hughes *et al.* 1997; Dean *et al.* 1999; Ritchie *et al.* 2011) describe the Corona Ridge as comprising one or two linear NE-SW-trending basinal highs, totalling *c.* 100-150 km in length, bound by NE-SW-striking faults, and delineated only by the Victory Lineament transfer zone (Rumph *et al.* 1993; Ebdon *et al.* 1995; Ritchie *et al.* 2011). Within other publications the Corona Ridge is presented as a more complex structure with three structurally separate blocks (Fig. 1; Ellis *et al.* 2009). Ellis *et al.* (2009) interprets the Corona Ridge as one NE-SW-trending feature (Fig. 1) bound by NE-SW-striking faults, which bifurcates within quadrant 214 into two separate highs each extending towards quadrant 217, which bound the Sissal sub-basin (denoted as SB in Fig. 1). Within the study area however, according to Ellis *et al.* (2009), the Corona Ridge comprises one NE-SW-trending high (Fig. 1)

Recent publications investigating the crystalline basement structure within the FSB (e.g., Rippington *et al.* 2015; Schofield *et al.* 2017; Holdsworth *et al.* 2019; Peacock & Banks 2020) often focus on other prospective structural highs in the basin (e.g., the Rona Ridge). Publications which are focussed on the Corona Ridge itself (e.g. Hardwick *et al.* 2010) describe reprocessing methods to improve seismic imaging of the complex Corona Ridge. However, at the time of publication, no detailed maps showing the structural complexity of the Corona Ridge are published.

Although the characterisation along the southern Corona Ridge has improved through time due to the drilling of the three deep penetrating Rosebank exploration and appraisal wells (213/27-1Z, 213/27-2, 213/27-3Z), knowledge of the structural configuration, geology, and hydrocarbon prospectivity of the central-northern Corona Ridge is still enigmatic. The work presented here

shows that the along strike structural configuration of the Corona Ridge is much more complex than previously thought, as will be discussed below.

Data and Methodology

The main seismic data used for interpretation throughout this project, and shown here in Figs 5, 6, 7 & 8, is a broadband 3D seismic survey acquired by PGS (Petroleum Geo-Services) for Total E&P U.K. Ltd and partners in two phases; phase-1 in 2013 (Galloway) and phase-2 in 2015 (Corona) (Joseph *et al.* 2017). Key parameters of each acquisition phase are summarised in Table 1 and the area covered by the survey is shown in Fig. 1.

Data is displayed at zero phase negative standard (Sheriff & Geldart 1982) European polarity, with a downward increase in acoustic impedance (hard) corresponding to a negative amplitude (trough) displayed in red and a downward decrease in acoustic impedance (soft) corresponding to a positive amplitude (peak) displayed in blue. Near the Top Paleocene, at 3.5 s TWT (*c.* 3.5 km depth) the dominant frequency is 22 Hz, giving a vertical resolution of *c.* 37.5 m (assuming a velocity of 3300 ms^{-1} for the Paleocene; Rippington *et al.* 2015). Towards the base Cretaceous at 6.5 s TWT (*c.* 12 km depth) within the Flett sub-basin the dominant frequency drops to 8 Hz, giving a vertical resolution of *c.* 147 m (assuming a velocity of 4700 ms^{-1} for the Cretaceous; Rippington *et al.* 2015). Towards the base of the survey at 8 s TWT (*c.* 18 km depth) the dominant frequency drops further to *c.* 6 Hz, giving a vertical resolution of *c.* 270 m (assuming a velocity of 6500 ms^{-1} for the crystalline crust; Rippington *et al.* 2015). Seismic data extends down to 10 s TWT.

Three exploration wells drilled along the central-northern Corona Ridge were used throughout this study: 213/23-1 (Eriboll), 214/21a-2 (South Uist) and 213/23c-1V (North Uist). Well data was downloaded from the NSTA National Data Repository (NSTA 2022) where it is freely available. The wells within this paper were drilled as near-vertical exploration wells, and throughout this paper depths are quoted in Measured Depth (MD (m)), unless otherwise specified. We have completed a detailed reinterpretation of well data including end of well reports, wireline data, composite logs, image logs, core, and biostratigraphy (where available) to allow the wells to be

placed in stratigraphic context of the NE Atlantic Margin (see Jolley *et al.* 2021), and in particular in the context of detailed stratigraphy of the Rosebank Field (after Schofield & Jolley 2013).

Central-Northern Corona Ridge Exploration wells

213/23-1 (Eriboll)

213/23-1 (Eriboll) was the first well drilled along the Corona Ridge, in July 1998 by Mobil. The well targeted three stratigraphic intervals, the primary Mesozoic-age Eriboll oil prospect on the footwall of a tilted fault-block (Corona Ridge) with three-way dip closure, and two shallower secondary targets within the upper Paleocene (Solway prospect) and middle Eocene (Caledonia prospect) (213/23-1 Final Geological Well Report 1999). Pre-drill concerns regarding timing, migration, and lack of charge of the secondary targets were confirmed by the presence of water within the upper Paleocene Solway and middle Eocene Caledonia prospects. The well encountered Eocene to Paleocene strata, Cretaceous strata, a section postulated to be Triassic strata (referred to as 'Triassic?' in the end of well report) and Devonian–Carboniferous strata. No Jurassic strata was penetrated in the well (213/23-1 Final Geological Well Report 1999). According to the end of well report, 213/23-1 (Eriboll) penetrated 1.5 metres of rock assigned as Precambrian Lewisian gneiss before reaching TD at 4344 m MD. However, cuttings of the 1.5 metres of Lewisian basement are described within the end of well report as both 'crystalline and porphyritic' and to contain 'lithic fragments' (213/23-1 Final Geological Well Report 1999). Numerous oil shows were encountered within Upper Cretaceous, 'Triassic?', and Devonian–Carboniferous strata.

213/23-1 (Eriboll) – Paleocene to Eocene: Identification of the T40-T45 Colsay Member and Colsay units 1-4

Our reinterpretation of various types of well data (specifically biostratigraphy suggestive of depositional environments associated with Colsay unts 1 to 4) obtained from 213/23-1 has allowed sequences penetrated within the well to be assigned to the current Paleocene–Eocene

lithostratigraphic framework (Ritchie *et al.* 2011; Schofield & Jolley 2013) and T-sequences (Ebdon *et al.* 1995) used throughout the FSB (Fig. 4), not assigned at the time the well was drilled.

By re-evaluating biostratigraphy, we found that the Horda Formation (sequence T60, Ypresian-age), not previously identified, lies conformably on the Balder Formation (sequence T50) which comprises claystone with thin beds of volcanic tephra. The upper Paleocene Solway prospect was prognosed between the Balder and Flett Formation. The Solway prospect, thought to be hosted in shallow marine sandstones, was also found to be dry (213/23-1 Final Geological Well Report 1999).

We found that the well (213/23-1, Eriboll) encountered 422 m of Flett Formation, more than double the original thickness interpreted post-drill (194 m) (Fig. 9a). No oil shows were observed within the 42 m thick upper section of the Flett Formation which we assign to the Hildasay Member (sequence T45). The well (213/23-1) penetrated a 380 m thick section we assign to the Colsay Member (sequence T40-T45) of the Flett Formation, which is comparable in thickness to the Colsay interval throughout the Rosebank Field (*c.* 400 m; 213/27-1 & 1Z End of Well Report 2004; 213/27-2 End of Well Report 2007). Within 213/23-1 (Eriboll) the Colsay interval is described in the end of well report as a series of sandstones interbedded with mudstones and siltstones (213/23-1 Final Geological Well Report 1999). Numerous traces of residual oil within the lower (sequence T40) Colsay Member were observed (Fig. 10).

According to the end of well report, the well (213/23-1) encountered Lamba Formation (sequence T36-T38) and an undifferentiated Paleocene-aged tuffaceous unit below the Flett Formation (Fig 9a) (213/23-1 Final Geological Well Report 1999). However, our biostratigraphic reinterpretation suggests both intervals actually represent the T40 Colsay 4 unit interval (Fig. 10) and that no T10-T38 sequences are present within the well. The Colsay 4 unit is comprised of material eroded and reworked from Paleocene-aged (sequence T10-T38) sediments.

Reinterpretation of the Colsay Member (sequence T40-T45) within 213/23-1 (Eriboll) using the end of well report, composite log, biostratigraphy, and resistivity image logs has facilitated the identification of a series of sequence T40 volcanic rocks, sub-basaltic, and intra-basaltic sandstones.

Biostratigraphic interpretation of two Rosebank wells (appraisal well 213/27-2 and exploration well 213/27-3Z) was used to correlate the Colsay intervals 21.3 km along the central-northern Corona Ridge from the Rosebank Field to 213/23-1 (Eriboll) (Fig. 11). Descriptions of each Colsay unit (1-4) within 213/23-1 are given within Table 2.

213/23-1 (Eriboll) – Paleocene to Eocene: Identification of T40-T45 Colsay Member volcanic intervals

According to the original composite log, two 2 to 3-metre-thick sections of 'intrusive volcanics' identified as 'dolerite? volcanics?' were penetrated between 2870-2890 m MD (2840-2860 m TVDSS) (Figs 9 & 10), within an 18 m thick limestone host rock. Cuttings of the 'intrusive volcanics' are described within the composite log as 'black-grey, translucent, opaque, brown, locally green, black mafic groundmass, hard, crystalline to very finely crystalline, equigranular, trace mica and pyrite, no porosity', however, a core plug taken within the upper 'intrusive volcanic' section is contrastingly identified as claystone in the end of well report (213/23-1 Composite Well Log 1998; 213/23-1 Final Geological Well Report 1999). Core plugs taken within the proposed limestone section are also contrastingly identified as siltstone and dolerite within the end of well report (Fig. 10). As a result of these discrepancies, we reinterpreted lithologies throughout the entire Colsay Member (T40-T45) interval using wireline, composite log, core plug, core, and resistivity image log data (Fig. 10). We interpret four volcanic intervals (Fig. 10) which were previously interpreted as either sandstone or limestone intervals in the original composite logs (213/23-1 Composite Well Log 1998).

The reinterpreted volcanic intervals are typified by low gamma ray values and fast sonic values (Fig. 10). Resistivity image logs of the volcanic intervals contain *c.* 10 cm wide conductive zones which likely represent open fractures or cooling joints (Fig. 10c & 10e), whilst other volcanic intervals (Fig. 10a & 10c) have thinner (<1 cm wide) vertical conductive (open) fractures (possibly drilling-induced). The thickness of laminated claystone overlying the volcanic intervals appears to be influenced by the underlying rough top surface of lava observed within image logs (Fig. 10f), suggesting the intervals within 213/23-1 (Eriboll) are lava flows, not igneous intrusions as suggested

for the two 2 to 3-metre-thick sections described as 'intrusive volcanics' within the original composite log (Fig. 10) (213/23-1 Composite Well Log 1998).

213/23-1 (Eriboll) – Cretaceous

Petrophysical analysis completed by Mobil suggests Upper Cretaceous Cenomanian–Turonian Shetland Group sandstones are oil bearing and contain 4.9 m of net pay (213/23-1 Final Geological Well Report 1999). No oil shows were recorded within the 19.5 m thick Lower Cretaceous Cromer Knoll Group. Lower Cretaceous claystone lies uncomformably on strata identified as 'Triassic?' (213/23-1 Final Geological Well Report 1999).

213/23-1 (Eriboll) – Does 213/23-1 penetrate a Triassic sequence?

The Triassic interval (*c.* 3585-3763 m MD) is assigned with uncertainty according to the end of well report and is referred to as 'Triassic?', although there is no biostratigraphic evidence for the assignation of a Triassic age to this section. The original biostratigraphic analysis states that 'palynological evidence suggests Carboniferous aged sediments may be present, but the results are not conclusive', in regard to the section assigned 'Triassic?' (213/23-1 Biostratigraphy Report 1999, p. 3). Within the 'Triassic?' section, (at 3736 m MD, Fig. 12) '*in situ* Carboniferous taxa' are recorded, although considered sparse and the interval remained lithostratigraphically unassigned as such (213/23-1 Biostratigraphy Report 1999, p. 45). Two separate interpretations of the interval are provided in the post-well biostratigraphic analysis: either a continuation of the Lower Cretaceous Cromer Knoll Group or the section being middle Carboniferous in age (213/23-1 Biostratigraphy Report 1999, p. 2). A continuation of Lower Cretaceous strata is unlikely due to the seismic observation that the Cromer Knoll Group lies at an apparent angular unconformably to the proposed 'Triassic?' section (Fig. 6). The absence of any unconformity within resistivity logs at and proximal to the proposed 'Triassic?'-middle Carboniferous boundary (pink dashed line, 3763 m MD; Fig. 12a) and the similarity of facies and bedding (orientation and dip) within the both the 'Triassic?' and middle Carboniferous section suggests that the 'Triassic?' section may instead be a continuation

of underlying middle Carboniferous strata (213/23-1 Final Geological Well Report 1999). We therefore interpret the 'Triassic?' interval within 213/23-1 (Eriboll) as a continuation of the underlying middle Carboniferous Clair Group strata identified within the original end of well report (Fig. 13) and discuss the section below.

213/23-1 (Eriboll) – Carboniferous

The middle Carboniferous (Clair Group) is described within the end of well report as a series of homogenous sandstones with good (*c.* 15%) porosities, conglomerates, laminated mudstones, and one 5 m thick interval of coal (213/23-1 Final Geological Well Report 1999). Fining up sequences containing flat to low-angle bedding and cross-bedding with localised mud clasts and burrows are evident within core obtained from the interval (213/23-1 Sedimentology & Petrography 1999). We interpret the presence of coal, laminated mudstones, conglomerate, and cross-bedded sandstones containing mud clasts and burrows to be deposited within a fluvial depositional environment (213/23-1 Sedimentology & Petrography 1999). Coal is also present within the age equivalent fluvial-fluviodeltaic Carboniferous sequences of the Clair Field (Robertson *et al.* 2020). Post-drill petrography of middle Carboniferous core (Fig. 12) suggests lower porosities (<2.5%) are present, the result of *c.* 1-metre-thick sections exhibiting extensive dolomite and calcite cement (Fig. 12) and the presence of matrix clay and quartz overgrowth cement (213/23-1 Sedimentology & Petrography 1999). Oil shows were encountered within the middle Carboniferous interval, with oil described as 'bubbling' from core (Fig. 12) (213/23-1 Final Geological Well Report 1999) and traces of oil were seen in mud at the shakers (3876-3884 m MD) (213/23-1 Final Geological Well Report 1999).

Lower Carboniferous strata are characterised within the composite log by sandstones with fair to good porosity, recorded to contain oil shows (213/23-1 Composite Well Log 1998). No image logs or core were obtained through the lower Carboniferous section. Average petrophysical properties throughout the Carboniferous section are shown in Table 3.

Despite some Carboniferous fractures (Fig. 12) exhibiting residual brown and black oil stains, the reservoir quality of the unit is considered poor due to the presence of dolomite cement, calcite

cement and clay smears (213/23-1 Sedimentology & Petrography 1999). We interpret fractures present within resistivity image logs of the middle Carboniferous strata to have dominant strike orientations of NE-SW and ENE-WSW (Fig. 12b). Fracture density is higher within the uppermost section of the middle Carboniferous (1 m^{-1}) previously interpreted as 'Triassic?' (3585-3763 m MD) compared with the lowermost middle Carboniferous section (0.5 m^{-1}, 3763-3884 m MD), although borehole washouts impair image log interpretation within the lower section (Fig. 12). We interpret borehole breakouts with NE-SW orientations and drilling-induced tensile fractures (DITFs) with NW-SE orientations within middle Carboniferous strata to suggest a present-day maximum horizontal stress (SHmax) orientation of NW-SE.

A DST was later performed on the lower to middle Carboniferous prospective 'Eriboll Middle Zone' from depths 3814-3914 m MD (Figs 9a & 13) after re-entry in August 1999, almost 9-months after the well was initially suspended (213/23-1 Final Geological Well Report 1999). The DST perforated 100 m of the Clair Group from which the 6.5 m of 'oil-bubbling' core had been recovered the previous year (Fig. 13). The DST produced only water and did not flow oil to surface, with no technical issues reported during the DST (213/23-1 Well Site Test Report 1999).

213/23-1 (Eriboll) – Devonian

The Devonian Lower Clair Group (interpreted post-drill as Upper to Middle Old Red Sandstone, Fig. 13) is described as fine to coarse grained, moderately-sorted sandstone with poor porosity and poor oil shows within the end of well report (213/23-1 Final Geological Well Report 1999). No image logs were obtained within the Devonian interval of 213/23-1 (Eriboll) (Fig. 13). Average petrophysical properties throughout the Devonian section are shown in Table 3.

Post-drill interpretation of wireline data by Mobil suggested a significant oil column was present in the Devonian–Carboniferous sequences, with average net-to-gross (NTG) of 42% and high water saturation (Sw) of 71% (213/23-1 Final Geological Well Report 1999, p. 7).

214/21a-2 (South Uist)

Well 214/21a-1 was drilled as part of a licence commitment in February 2008 by Shell and partners to target the South Uist gas prospect, located along an elongated (*c.* 4 km by 10 km) four-way dip-closed structure (Figs 15b & 16b), around 10 km from the Corona Ridge structural high (214/21a-2 End of Well Report 2010). Pre-drill in place estimates were 2.1 trillion cubic feet of gas (P.799 Relinquishment Report 2014). After extended operations challenges (e.g., BOP repairs and waiting on weather) the well was suspended and re-drilled as 214/21a-2 (South Uist) in July 2009 (214/21a-2 End of Well Report 2010). Before drilling, prognosed risks and uncertainties were absence of reservoir and the age of the target interval, which was debated by the well partners. Shell interpreted the target interval as the lower Paleocene Sullom Formation (T20); however, partner ConocoPhillips interpreted the target as Maastrichtian-age Cretaceous sedimentary rocks (214/21a-2 End of Well Report 2010). On drilling, the Sullom T20 target was encountered 173 m above the prognosed target depth. The target interval (>3713 m MD) consisted of Cretaceous mudstone and limestone stringers with no sandstones present, proving the stratigraphic interpretation of ConocoPhillips to be correct (214/21a-2 End of Well Report 2010).

213/25c-1V (North Uist)

213/25c-1V was drilled by BP over 295 days from March 2012 to January 2013, 12 km NW of South Uist, to fulfil licence commitments agreed with the regulator. The well was designed to test the Devonian–Carboniferous and/or Jurassic North Uist oil prospect estimated to contain 1067 mmboe in place (pre-drill P50 case, P.1192 Relinquishment Report 2017) within a three-way tilted fault-block sealed by Jurassic and Cretaceous mudstones, with the reservoir prognosed at 4057 m MD (213/25c-1V End of Well Report 2013). A secondary stratigraphic Paleocene target, the 430 mmboe in place (pre-drill P50 case, P.1192 Relinquishment Report 2017) Cardhu prospect, was prognosed to lie beneath the Balder Formation at 3062 m MD (213/25c-1V Geological Operations Report 2013). Operational challenges were encountered whilst drilling the well (see Watson *et al.* 2019), contributing to a rig mobilisation of 312 days and costs estimated at >100 million GBP (Energy Voice 2012; 213/25c-1V End of Well Report 2013). The well proved the presence of condensate within the

Carboniferous Upper Clair Group and encountered Eocene to Devonian-age strata, including rocks of early to middle Jurassic-age, before terminating at 4776 m MD within Devonian strata.

213/25c-1V (North Uist) – Paleocene to Eocene

The T60 middle Eocene Stronsay Group comprises mudstone with massive (*c.* 50 m thick) interbeds of sandstone. Beneath the Stronsay Group the Balder Formation was encountered and is described as tuffaceous mudstone with siltstones, trace sandstone and trace limestone within the end of well report (213/25c-1V End of Well Report 2013). Although not prognosed, an 8 m thick (sub seismic resolution) section of the Flett Formation was encountered within the secondary target (Cardhu) interval beneath the Balder Formation. Within 213/25c-1V (North Uist) the Flett Formation is described as predominantly mudstone, with traces of sandstone observed as rock flour in cuttings. Although also not prognosed, the Lamba and Vaila Formations were both penetrated below the Flett Formation (213/25c-1V Composite Well Log 2013). The Vaila Formation lies unconformably on the Upper Cretaceous Shetland Group.

213/25c-1V (North Uist) – Cretaceous and Jurassic

According to the composite log, the Upper Cretaceous strata consists of mudstone, siltstones, and occasional limestone stringers (213/25c-1V Composite Well Log 2013). In 213/25c-1V (North Uist) oil shows were observed solely within cuttings from the Santonian Shetland Group at 3460 m MD. The section containing oil shows was drilled with oil-based mud (OBM), and as oil show fluorescence was similar to that of the OBM fluorescence shows were inconclusive. Lower Cretaceous strata are characterised by mudstone with limestone stringers and thin sandstones. The Lower Cretaceous lies unconformably on Lower to Middle Jurassic strata. Jurassic strata are characterised by organic-rich mudstones. The 68.8 m thick Jurassic section lies unconformably on the Carboniferous Upper Clair Group (UCG).

213/25c-1V (North Uist) – Devonian to Carboniferous

Within the composite log, the Carboniferous UCG is characterised by sandstones with mudstone interbeds (213/25c-1V Composite Well Log 2013). The lower, Devonian–Carboniferous section of the Clair Group comprises sandstone, siltstone, and thin mudstones. Sedimentological observations of the Devonian–Carboniferous Clair Group are comparable to 213/23-1 (Eriboll), suggesting a fluvial depositional environment, although this is speculative due to the lack of conventional (continuous) core obtained in 213/25c-1V (North Uist).

213/25c-1V (North Uist) discovered gas condensate (42.5 API; P.1192 Relinquishment Report 2017) in two reservoirs, the upper (Carboniferous, 3974-4069 m MD) and lower (referred to as Devonian/Carboniferous within the end of well report, 4069-4773 m MD) Clair Group reservoirs (Fig. 9b). No gas-water contact (GWC) was identified in the composite log or end of well report, although neutron-density crossover implies a GWC at *c.* 4630 m MD. The much thicker (704 m) lower reservoir is referred to as 'tight', with very low mobilities (<0.1 mD/cP) suggestive of low permeabilities which alongside high Sw (82%), resulted in no net pay interpreted by BP within the lower reservoir. Properties of the upper and lower reservoirs are shown in Table 3.

Before drilling, the upper reservoir (North Uist discovery) was estimated to contain 104 mmboe (P50 case) of condensate in place, just under 10% of the pre-drill in place P50 estimates (1067 mmboe) (P.1192 Relinquishment Report 2017). No well testing was performed, and the well was plugged and abandoned.

Seismic interpretation along the Central-Northern Corona Ridge

Top Crystalline Basement time–structure maps (Fig. 14) show the central-northern Corona Ridge as one structurally high (at *c.* 5 s depth TWT) feature within the SW of the study area, which splits into two structural highs towards the NE which have less relief (*c.* 6 s depth TWT). The southerly branch splits further into two components, creating a series of lows between the highs of crystalline basement within the NE of the dataset (Fig. 14b). The Corona Ridge is bound by a series of mapped normal faults which strike NE-SW (collectively termed the Flett-Corona Fault; Rippington *et al.* 2015) within the Flett sub-basin. Two faults that strike N-S and NNW-SSE (red faults, Figs 5 & 14),

oblique to the main series of NE-SW-striking faults (Fig. 14), are mapped within the centre of the dataset, where the Corona Ridge bifurcates. The time–structure map of the Top Crystalline Basement (Fig. 14) horizon clearly shows that the structure of the Corona Ridge is far more complex than previous interpretations (see Fig. 14b for comparison). Down-flank fault terraces of Jurassic and/or Devonian–Carboniferous strata (Figs 7, 15a & 16a) were also identified, downthrown from the main Corona Ridge structure along the Flett-Corona Fault, which are overlain by Cretaceous and/or Jurassic sedimentary rocks.

Towards the base of the seismic survey (between 7-9 s TWT) a series of high amplitude, hard (red, trough), semi-continuous reflections (Fig. 5) can be observed beneath the central-northern Corona Ridge (labelled on Figs 5 & 7). The high-amplitude reflections appear to coalesce and have upwards concave geometries. The high-amplitude reflections are present at these depths throughout most of the 3D survey, although a much higher quantity is present in the centre of the 3D seismic dataset (e.g. Fig. 5) compared with the northern part of the dataset where there are none (Fig. 8). Assuming velocities based on Rippington *et al.* (2015) for the crystalline continental crust, this would place these reflections at *c.* 16 to 20 km depth. The minimum vertical resolution at *c.* 18 km depth (*c.* 8 s TWT) is *c.* 270 m.

Based on our mapping of the Faroe-Shetland Sill Complex, emplacement of magma into Cretaceous and lower Paleocene sedimentary host rocks was generally confined to the Flett and Sissal sub-basins (Fig. 17). Only two igneous intrusions were interpreted within the seismic data to have been emplaced within Cretaceous host rock above the central-northern Corona Ridge (Figs 5 & 17), implying a lack of magma emplacement.

Discussion

Crystalline basement structure of the central-northern Corona Ridge

Whilst the crystalline basement rocks of the Rona Ridge have been extensively studied (due to the Clair Field and other basement plays (e.g., Bonter & Trice 2019; Holdsworth *et al.* 2019)), the Corona Ridge has received much less attention, and there are currently no detailed crystalline

basement maps published. Work along the Corona Ridge has largely focused on prospectivity within overlying strata (e.g., Paleocene–Eocene plays; Hardman *et al.* 2018; Duncan *et al.* 2020) and tends to adopt simplified structural maps of the Corona Ridge. The NE-SW-trending structure of the central-northern Corona Ridge mapped as part of this study (Fig. 14b) shows that its structure is more complex than older, poor, sub-basaltic seismic imaging previously allowed authors to image (e.g., Hughes *et al.* 1997; Ellis *et al.* 2009). Previous interpretations show the structural high as one crystalline block within the study area (see map bottom right, Fig. 14b), we show that instead the central-northern Corona Ridge splits into three structural highs towards the NE, creating a series of lows (mini-basins, Fig. 14a) between the highs of crystalline basement. We also show that the NE-SW-striking Corona Ridge bounding normal faults (Fig. 14), often simplified as one feature within regional maps of the basin (e.g., Mudge & Rashid 1987; BGS 1996; Ellis *et al.* 2009; Ritchie *et al.* 2011) and collectively termed the Flett-Corona Fault by Rippington *et al.* (2015), are constituted of a series of discrete faults which should instead be termed the Flett-Corona Fault System.

Oblique faults and down-flank terraces of the Corona Ridge

The two N-S and NNW-SSE-striking faults (red faults; Figs 5, 14 & 15a) mapped within the centre of the study area are oblique to the NE-SW-striking of basement bounding faults of the collectively termed Flett-Corona Fault System. The 'oblique' faults are expressed at both the Top Crystalline Basement and Base Cretaceous levels (red faults; Figs 5, 14 & 15a) and are located where the Corona Ridge is interpreted to bifurcate into two parts mapped within the NW of the dataset. Although much of the NE-SW-striking structural fabric in the FSB (and indeed broader NE Atlantic Margin) is thought to reflect inheritance from pre-existing crystalline basement trends, the N-S-striking oblique faults do not appear to reflect structural inheritance from either NW-SE-trending Precambrian shear zones (Knott *et al.* 1993), NE-SW-striking Caledonian compressional fault systems (Doré *et al.* 1997) or NW-SE-trending lineaments or 'transfer zones' (Rumph *et al.* 1993; Moy & Imber 2009). Dean *et al.* (1999) also map two dominant fault trends on the Corona Ridge (at Base Cretaceous level, referred to as Base Upper Cretaceous within Dean *et al.* 1999), with N-S and

NE-SW-striking orientations and postulate that the N-S faults are Jurassic in age. Obliquity of the N-S and NNW-SSE-striking faults from dominant NE-SW-striking structural fabrics is also observed across parts of the NE Atlantic Margin, including the North Viking Graben, Porcupine Basin and Møre Margin (Doré *et al.* 1997; Schiffer *et al.* 2020).

N-S-striking rift basins within the NE Atlantic are thought to have originated either during E-W-directed Triassic–Jurassic extension, which exploited late Caledonian structures, or as a new trend established from northwards rift propagation during the early Cretaceous (Dean *et al.* 1999; Schiffer *et al.* 2020). It has also been suggested that the N-S structural trends seen across the NE Atlantic Margin may reflect the reactivation of Pre-Caledonian or Caledonian suture zones, although direct evidence for this is sparse (Schiffer *et al.* 2020). Assessing the origins of oblique faults mapped here (red faults; Figs 5, 14 & 15a) and any further extent of N-S-striking faulting across the FSB is challenging, as the imaging of basement structures are often obscured by overlying Paleogene lava flows and the Faroe Shetland Sill Complex (Hardwick *et al.* 2010). However, the identification of N-S structuration within the crystalline basement of the central-northern Corona Ridge suggests that such features could be more extensive than previously realised within the basin.

Down-flank fault terraces of Jurassic and/or Devonian–Carboniferous strata (Figs 7, 15a & 16a) overlain by Cretaceous and/or Jurassic sedimentary rocks were also identified downthrown from the main Corona Ridge structure along the Flett-Corona Fault System. Barr *et al.* (2007) describes several similar terraces which extend the Clair Field from the main Rona Ridge structure, also comprising Devonian and Jurassic strata (referred to as the Clair South development; Robertson *et al.* 2020).

High-amplitude reflections beneath the central-northern Corona Ridge

A series of hard (red, trough) high amplitude reflections are observed within the 3D seismic data (Figs. 5 & 7), beneath the central-northern Corona Ridge between 7 and 9 s TWT (*c.* 16 to 20 km). The high-amplitude reflections have upwards concave geometries and appear to often coalesce with other high amplitude reflections. The minimum vertical resolution at *c.* 18 km depth (*c.* 8 s TWT) is

c. 270 m. Seismic refraction data and associated velocity modelling within the study area (e.g., iSIMM, Mobil-1 & Mobil-2 lines; White *et al.* 2005; Makris *et al.* 2009; Roberts *et al.* 2009) indicate that the depth to the Moho beneath the Corona Ridge is *c.* 17-20 km (Funck *et al.* 2017; Petersen & Funck 2017). It is therefore likely that the high amplitude reflections are located within the lower crust.

Whilst there is no direct evidence as to the origin of these high amplitude reflections, through comparison with analogous high amplitude reflections published throughout the NE Atlantic Margin which have the same reflectivity, geometries, and are located at similar depths (*c.* 15km, White *et al.* 2008; *c.* 7-9 s TWT, Abdelmalak *et al.* 2017 and Wrona *et al.* 2019), we tentatively propose that the high amplitude reflections could be caused by basic intrusive bodies within the lower crust.

Devonian–Carboniferous Clair Group

The Clair Field, located on the Rona Ridge (*c.* 70 km from the central Corona Ridge), is expected to produce over 940 million barrels of oil from Devonian–Carboniferous Clair Group reservoirs (Robertson *et al.* 2020). The discovery of 104 mmboe in place (post-drill P50 case) of condensate in North Uist (213/25c-1V), proves that the Devonian–Carboniferous is a working play on the Corona Ridge (P.1192 Relinquishment Report 2017). However, no well tests were performed within 213/25c-1V, which limits the interpretation of reservoir volume and accurate estimation of post-drill connected in-place volume of North Uist.

Remnants of an intermontane basin are mapped on the Corona Ridge (Fig. 14b) which contains Devonian–Carboniferous strata penetrated by 213/23-1 (Eriboll) and 213/25c-1V (North Uist) (Fig. 16a). We also note the presence of the Clair Group below the Rosebank Field to the SW of the study area, confirmed by wells 213/27-1Z (95.8 m) and 213/27-2 (90 m) (Fig. 1b) (213/27-1 & 1Z End of Well Report 2004; 213/27-2 End of Well Report 2007). The intermontane basin possibly present along the Corona Ridge throughout the Devonian to Carboniferous is perhaps analogous to the Clair Basin located on the Rona Ridge (Ritchie *et al.* 2011; Smith & Ziska 2011). No Devonian–Carboniferous Clair Group was reported to have been penetrated to the NE of the study area in well 214/09-1 (Bunnehaven, Fig. 1b), and hence most previous work (e.g., Smith & Ziska 2011;

Stoker *et al.* 2014) does not extend its distribution north of 213/25c-1V (North Uist). Smith & Ziska (2011) interpret 213/23-1 (Eriboll) as the only well to penetrate the entire Devonian–Carboniferous sequence on the Corona Ridge (totalling 753 m) before terminating in crystalline basement. The lack of penetrations of the entire Devonian–Carboniferous sequence on the Corona Ridge compared with the Rona Ridge does not allow for comparison of thicknesses across the two ridges. However, our mapping of the thickness of the Devonian–Carboniferous sequences (Fig. 16a) does reflect varying thicknesses of Devonian–Carboniferous strata (0-1.6 s TWT), comparable to the variable thicknesses within the Clair Field (*c.* 150-900 m, Robertson *et al.* 2020) and Rona Ridge as a whole (*c.* 1000 m, Ziska & Anderson 2005).

Early Clair Field wells (drilled from 1977-1985) failed to confirm economical amounts of recoverable hydrocarbons within the Clair Group on the Rona Ridge (Robertson *et al.* 2020). Ogilvie *et al.* (2015) attributes the low flow rates (<1000 BOPD) observed in early appraisal drilling to vertical wells being unlikely to penetrate potentially productive open fractures, compared with later stage horizontal well sections (i.e., during the 1990s) which penetrated vertical fractures, proving that required flow rates could be achieved. We note that well 213/23-1 (Eriboll), much like early Clair Field appraisal wells, had a vertical trajectory and was therefore not orientated optimally to intersect any open fracture sets that may be present. The DST performed within 213/23-1 (Eriboll) also tested only 100 m of lower to middle Carboniferous strata, which is 10% of the length needed to obtain successful flow rates (18 000 BOPD) from a 950 m horizontal section within the later stage Clair Field appraisal wells (206/8-10 and 206/8-10z, Fig. 1b; Robertson *et al.* 2020). Core obtained within the tested interval of 213/23-1 (Eriboll) (Fig. 12c) exhibits evidence for abundant calcite cementation and is not representative of the 753 m thick Devonian–Carboniferous section which showed positive early signs of oil present (3876-3884 m MD, e.g., positive flow tests and oil shows 'bubbling' from core). We therefore suggest that Eriboll may be under appraised.

Devonian–Carboniferous Clair Group: Is there fracture enhanced permeability along the central-northern Corona Ridge?

According to critical stress theory, fractures optimally orientated in relation to the present-day stress field (usually parallel to the orientation of SHmax) are more likely to be hydraulically conductive and thus potentially allow the transmission of fluids (Hillis 1997; Rogers 2003; Tassone *et al.* 2017). On the central-northern Corona Ridge we interpret an SHmax orientation of NW-SE, which is consistent with general trends of present-day maximum horizontal stress observed across NW Europe (Holford *et al.* 2015). Therefore, according to critical stress theory, NE-SW & ENE-WSW-striking Carboniferous fractures we interpret within 213/23-1 (Eriboll) (Fig. 12) are not optimally orientated for enhanced fracture permeability, much like the Carboniferous strata of the Clair Field on the Rona Ridge (Robertson *et al.* 2020).

Within the Devonian Lower Clair Group reservoir of the Clair Field, according to Robertson *et al.* (2020), enhanced fracture permeability has been instrumental in achieving commercial flow rates. In contrast to the Clair Field, only poor oil shows were encountered within Devonian strata penetrated by 213/23-1 (Eriboll), subsequently no image logs were obtained, and no DST was completed within the Devonian section of 213/23-1, which precludes the analysis of any potential fracture permeability which may be present within Devonian strata along the central-northern Corona Ridge.

Absence of Triassic on the Corona Ridge: extending the Devonian–Carboniferous play

Less than two years after Mobil drilled 213/23-1 (Eriboll) in 1998, ExxonMobil drilled 214/09-1 (Bunnehaven, Fig. 1b) 92 km to the NE along the Corona Ridge, continuing to chase the 'pre-rift' section. No Devonian–Carboniferous strata were reportedly penetrated within 214/09-1 (Bunnehaven), although the well penetrated a 73 m thick 'indeterminate' interval unconformably overlying Lewisian Crystalline Basement which, like the proposed 'Triassic?' interval in 213/23-1 (Eriboll), was barren of *in situ* microfossils (214/09-1 Post-Drill Well Summary 2001). The indeterminate interval within 214/09-1 (Bunnehaven) was characterised by claystones, sandstones, dolomite, and gneissic conglomerates, comparable to the interval re-interpreted as middle Carboniferous within 213/23-1 (Eriboll) previously assigned as 'Triassic?' (see Fig. 12c, core 4;

214/09-1 Post-Drill Well Summary 2001). The nearest Triassic penetration to the Corona Ridge is 80 km away, to the SE on the Rona Ridge (206/05-2, Fig. 1b), with these strata described as red beds with reddish brown claystone and occasional fragments of hard limestone (206/5-2 Final Geological Report 1996); none of these lithologies are described in either 213/23-1 (Eriboll) or 214/09-1 (Bunnehaven) (Fig. 1b).

Triassic strata in the FSB are typically entirely barren of all fossil groups (Swiecicki *et al.*1995). According to Morton *et al.* (2010) and Morton & Milne (2012), the Devonian–Carboniferous strata of the Clair Field are also entirely barren, making age determination between Triassic and Devonian–Carboniferous sections challenging. Age determination of the Carboniferous UCG section in 213/25c-1V (North Uist) using biostratigraphic and heavy mineral data was also challenging according to the end of well report, comparable to the challenges associated with the proposed 'Triassic?' interval in 213/23-1 (Eriboll) and indeterminate interval in 214/09-1 (Bunnehaven).

The distribution of Permian–Triassic rocks in the central FSB (e.g., Quinn & Ziska 2011; Stoker *et al.* 2014; Stoker *et al.* 2017b) is inferred solely upon two proposed well penetrations, 213/23-1 (Eriboll) and 214/09-1 (Bunnehaven) (Fig. 1b). Our interpretation of the absence of Triassic strata from 213/23-1 (Figs 12 & 13), alongside the absence of Triassic strata from other areas of the Corona Ridge (213/25c-1V, North Uist and 213/27-1Z, Rosebank) casts doubt on the interpretations of Triassic presence within 214/09-1 (Bunnehaven, Fig. 1b) (Quinn & Ziska 2011; Stoker *et al.* 2014; Stoker *et al.* 2017b) and therefore from the central FSB, with penetrations of Triassic strata possibly confined solely to the present-day margins of the FSB within the Judd (204/29-1) sub-basin and the Westray High (204/19-1 and 204/19-9) (Fig. 1b) (see Štolfova & Shannon 2009).

If like 213/23-1 (Eriboll), the indeterminate interval in 214/09-1 (Bunnehaven) is Devonian–Carboniferous in age and not Triassic (or Jurassic), this could provide renewed potential for the presence of exploration plays of this age (provided there is Devonian enhanced fracture permeability and large enough structural closures) along the northern Corona Ridge and the possible presence of gas-prone source rocks (Carboniferous coals, Fig. 2) which have not been previously interpreted this

far north (Quinn & Ziska 2011; Stoker *et al.* 2014; Stoker *et al.* 2017b). This may also have wider implications for the understanding of early geological evolution of the FSB subsequent to post-Caledonian orogenic collapse, as Devonian–Carboniferous depositional systems may have been far more extensive than previously thought within the north of the FSB (Stoker *et al.* 1993; Nichols 2005; Smith & Ziska 2011).

Our interpretation of no Triassic strata present within 213/23-1 suggests an unconformity between middle Carboniferous and Lower Cretaceous strata of at least a *c.* 154-million-years. Implications of our interpretation, the absence of Triassic strata, are that either; (1) Permian–Triassic rocks were deposited but then eroded from the Corona Ridge and recycled into the adjacent Corona, Flett and Sissal sub-basins as syn-rift reservoir units throughout the late Jurassic to early Cretaceous evolution of the Corona Ridge or, (2) no Permian–Triassic rocks were deposited as the Corona Ridge was a prominent structural high throughout the Permian–Triassic.

Although the interpretation of Permian–Triassic strata being eroded during the late Jurassic to early Cretaceous development of relief along the Corona Ridge (Ritchie *et al.* 2011; Hardman *et al.* 2018) is supported by the lack of Permian to Jurassic strata within 213/23-1, the preservation of Lower to Middle Jurassic within 213/25c-1V (North Uist) and Upper Jurassic-age strata within 213/27-1Z does not support this interpretation (213/27-1 & 1Z End of Well Report 2004; 213/25c-1V End of Well Report 2013). If the latter interpretation is correct, the Corona Ridge may have been a structurally high feature during the Permian–Triassic (hence no deposition), which was then flooded during the proposed Jurassic marine incursion (Dean *et al.* 1999), and then re-emerge during the late Jurassic to early Cretaceous rift period which is understood to be largely responsible for the present-day structure of the Corona Ridge (Ritchie *et al.* 2011; Hardman *et al.* 2018). During late Jurassic to early Cretaceous extension there may have been some localised shedding and recycling of Carboniferous and Jurassic strata from the Corona Ridge (forming localised syn-rift targets) into adjacent sub- and mini-basins (Figs 14 & 15a). This may explain the absence (in 213/23-1) and relatively thin (68.7 m in 213/25c-1V compared with 452 m penetrated in 213/27-3Z) presence of

Jurassic strata along the central-northern Corona Ridge (213/27-3Z End of Well Report 2009; 213/25c-1V End of Well Report 2013).

The Lower Cretaceous syn-rift play

The possible recycling of 'pre-rift' Devonian–Carboniferous, Permian–Triassic and Jurassic strata from emergent structural highs (such as the Rona Ridge; Clark *et al.* 2020), with the addition of extrabasinal sediment (Stoker & Ziska 2011), during widespread early Cretaceous extensional deformation is thought to be responsible for the deposition of Lower Cretaceous reservoirs of the Cromer Knoll Group, which act as reservoirs for the Edradour Field and Glendronach discovery (Stoker 2016; Clark *et al.* 2020). Evidence of this widespread early Cretaceous extension can be observed within Figs 7 & 8, where syn-sedimentary deposition of Cretaceous sediments appears to relate to normal faults. Within the West Shetland Basin, the Lower Cretaceous Victory Formation is also a proven gas reservoir for the Victory Field (Fig. 1b & 2) (Goodchild *et al.* 1999). Rift-related topography is thought to have controlled syn-rift depositional systems throughout the early Cretaceous along major relay ramps into inherited half-grabens (Larsen *et al.* 2010).

Recycling of Carboniferous and Jurassic strata during the late Jurassic to early Cretaceous emergence of the Corona Ridge (as discussed in the previous section) is possibly reflected by the thin presence of the Lower Cretaceous Cromer Knoll Group within 213/23-1 (Eriboll, Fig. 9a), 213/25c-1V (North Uist, Fig. 9b) and 214/09-1 (Bunnehaven) (*c.* 120 m; 214/09-1 Post-Drill Well Summary 2001), and the irregular occurrence of Jurassic rocks along the Corona Ridge (e.g. absent in 213/23-1 but present in 213/25c-1V and 214/09-1). Within neighbouring basins such as the Flett sub-basin, into which localised shedding of eroded sediment may have occurred from the Corona Ridge, Lower Cretaceous intervals are much thicker, reaching up to 1168 m (Stoker 2016). The Cretaceous significantly thickens (>2000 ms, Fig. 16b) from relief present along the central-northern Corona Ridge at the base Cretaceous level (Fig. 15a) into Cretaceous depocenters of the Sissal sub-basin and other mini-basins identified between the sections of the Corona Ridge within the NE of the dataset (mini-basins, Fig. 14b). This suggests that there may be the potential for packages of

Lower Cretaceous syn-rift plays to be present in the NE of the study area, with play fairways located off structural highs.

At the time of publication, no well has specifically targeted the Lower Cretaceous syn-rift play near the central-northern Corona Ridge within the sub-basins (Corona, Flett and Sissal) in and around the northern area of the FSB (Larsen *et al.* 2010; Stoker & Ziska 2011). In general, few wells have specifically targeted Lower Cretaceous strata in the northern FSB. Well 208/24-1A (NE part of the Flett sub-basin, Fig. 1b) encountered 64.7 m of Lower Cretaceous sandstone which contained no oil shows (Stoker & Ziska 2011). Wells which have encountered Lower Cretaceous sands within the northern FSB whilst targeting other intervals are confined to the Corona Ridge (214/09-1, Bunnehaven) and the Erlend High (209/12-1) (Fig. 1b). Thin Lower Cretaceous sands encountered in both wells (214/09-1 and 209/12-1, Fig. 1b) were only observed as rock flour at the surface. The bias resulting from wells drilled upon structural highs restricts the understanding of how syn-rift Lower Cretaceous reservoirs may be distributed within the deeper sub-basin areas such as the Corona, Flett and Sissal sub-basins. The possible distribution of Lower Cretaceous reservoirs is therefore largely implied by underlying structures (Figs 14 & 15a) which may have influenced the deposition of syn-rift Cretaceous sediments into structural lows off the Corona Ridge within the NE of the study area.

Igneous intrusions emplaced within Cretaceous strata along the central-northern Corona Ridge

There is a lack of igneous intrusion emplacement within the Phanerozoic sedimentary sequences directly above the central-northern Corona Ridge itself (Fig. 17). This contrasts with the Flett sub-basin where significant amounts of igneous intrusions have been emplaced within Cretaceous and lower Paleocene sedimentary rocks (Figs 7, 8 & 17). This possibly suggests that magma was less able to exploit the thick crust *via.* basement-bounding faults (e.g., Flett-Corona Fault System) during periods of Paleogene intrusive magmatism along the central-northern Corona Ridge, in comparison to the thinner crust of the basinal areas (Schofield *et al.* 2017).

Paleocene–Eocene: Colsay Member T40-T45 Prospectivity

Distribution of sequences T40-T45 along the central-northern Corona Ridge

Since the discoveries of the Cambo (discovered 2002) and Rosebank (discovered 2004) Fields, totalling *c.* 700 mmboe of recoverable resources, exploration and research focus has largely been confined to post-rift Paleocene to Eocene-aged reservoirs along the Corona Ridge (Smallwood & Kirk 2005; Austin *et al.* 2014; Loizou 2014; Siccar Point Energy 2020a). The Rosebank Field reservoir is within the upper Paleocene–lower Eocene-aged intra- and sub-basaltic Colsay Member (T40-T45) sandstones. During T40-T45 deposition of the Colsay Member a series of flood basalt (lava) sequences of the FIBG were also emplaced, forming intra-basaltic stratigraphic plays along the Corona Ridge (Jolley & Bell 2002; Passey & Jolley 2009; Hardman *et al.* 2018).

Along the Cambo High and within the south Rosebank Field, the T40-T45 interval has a very distinct seismic response, characterised by a series of stacked high amplitude reflections (Poppitt *et al.* 2018, p. 378, Fig. 6; Duncan *et al.* 2020, p. 985, Fig. 6) which are tied to individual T40-T45 Colsay units (Hardman *et al.* 2018, p. 77, Fig. 7a). Throughout most of the dataset used in this study, no similar Flett Formation seismic response is observed, except for the area south of 213/23-1 (Eriboll) (Fig. 5) which does not appear to correlate with areas of the thickest Flett Formation presence.

Schofield & Jolley (2013) proposed that, where a clastic intra-basaltic depositional system develops, lava-field morphology plays an important role in controlling and diverting sediment input, drainage systems and subsequent reservoir deposition within topographical lows in and around the margins of the lava fields. Understanding the structure present along the Corona Ridge (e.g., palaeo-highs and lows underlying sequence T40) prior to (Fig. 15b) and during (Fig 15c) the deposition of such complex sequences is also, according to Hardman *et al.* (2018), key to identifying sequence T40-T45 intra-basaltic play fairways within the central-northern Corona Ridge area. Our mapping of structures (Fig. 15) underlying such complex depositional systems and our identification of volcanic intervals previously missed within 213/23-1 (Eriboll) (Fig. 11) has facilitated a more detailed understanding of the possible distribution of T40-T45 intra- and sub-basaltic play fairways along the

central-northern Corona Ridge. Sequence T40 intra-basaltic Colsay sediment is thought to have predominantly been deposited within topographic lows (Schofield & Jolley 2013) parallel to palaeo-highs (NE-SW) present along the Corona Ridge, where drainage systems are thought to have developed (Hardman *et al.* 2018). This distribution of T40-45 sediments is also reflected within our mapping (Figs 15 & 16). The NW-SE trend present within the T40-T45 isochron (Fig. 16d) runs parallel to the central-northern Corona Ridge and is thickest within the topographic lows present at the near Top Palaeocene level (Fig. 15c). Significant thinning of the Flett Formation from 422 m within 213/23-1 (Eriboll) to 8 m within 213/25c-1V (North Uist) (over 18 km, Fig. 16d) also reflects the complex distribution of sequence T40-T45 along the Corona Ridge discussed by Schofield & Jolley (2013). This is possibly attributed to the palaeo-high present to the north of 213/25c-1V (North Uist) at the Top Cretaceous (Fig. 15b) and near Top Paleocene levels (Fig. 15c) which may have acted to divert sediment into the topographic low adjacent to the central-northern Corona Ridge.

Although published research has largely overlooked the possible distribution of intra- and sub-basaltic Paleocene–Eocene-aged (sequence T40) reservoirs NE of the Rosebank Field, an examination of prospectivity by OMV and partners *c.* 50 km north of the study area, within now relinquished licence area P1997 (Fig. 1b), suggests reservoir presence and quality is high risk within the Paleocene–Eocene Flett interval and that seismic imaging is too poor to allow calibration with offset wells (P.1997 Relinquishment Report 2015).

Extending the intra- and sub-basaltic plays of the Rosebank Field along the central-northern Corona Ridge

The reinterpretation of the Flett Formation within 213/23-1 (Eriboll) has facilitated the identification of four volcanic intervals and intra-basaltic and sub-basaltic sandstones of the Colsay Member (sequence T40-T45). These intervals were not previously interpreted within 213/23-1 (Eriboll) (213/23-1 Final Geological Well Report 1999) and were not previously thought to extend this far north along the Corona Ridge from the Rosebank area (Passey & Hitchen 2011; Hardman *et al.* 2018).

Biostratigraphic interpretation of two Rosebank wells (exploration well 213/27-3Z and appraisal well 213/27-2, Fig. 1b) was also used to correlate Colsay Member units (1-4) 21.3 km northwards along the central-northern Corona Ridge from the Rosebank Field (213/27-2 and 213/27-3Z) to those we have identified within 213/23-1 (Eriboll) (Fig. 11). To allow comparison of Colsay Member units, descriptions of the Colsay Member (sequence T40-T45) sandstone units (1-4) from within the Rosebank Field are provided within Table 2, alongside observations of the Colsay intervals we interpret within 213/23-1 (Eriboll).

The two main reservoirs of the Rosebank Field, the Colsay 1 unit and Colsay 3 unit, thin into 213/23-1 (Eriboll) from 213/27-3Z and contain more net claystone. However, the Colsay 2 unit and Colsay 4 units both thicken into 213/23-1 (Eriboll) from Rosebank and contain more net sandstone. Specifically, within 213/23-1, the Colsay 4 unit contains a 25 m thick sandstone which contains oil shows. Colsay 4 is an interval typically characterised by volcaniclastic siltstones and claystones within the Rosebank Field (Fig.11). The transition of T45 upper Colsay 1 unit palaeoenvironments from fully marine in Rosebank to shallow marine shelf in 213/23-1 (Eriboll) (Table 2) supports interpretations of a palaeo-coastline by Hardman *et al.* (2018) between Rosebank and 213/23-1 during the deposition of the T45 Colsay 1 interval (post volcanic rocks).

Log signatures of the four volcanic intervals (Fig. 10) we interpret within the Colsay Member section of 213/23-1 (Eriboll) are not representative, as suggested within the composite log ('intrusive volcanics'; 213/23-1 Composite Well Log 1998), of igneous intrusions encountered within the FSB as described by Mark *et al.* (2018b, p. 741, Fig. 6). Instead, the intervals have comparable log characteristics with lavas present across the FSB as described by Nelson *et al.* (2009) and Watson *et al.* (2017) and are reinterpreted as such by this study (Fig. 10). The four intervals of volcanic rocks we interpret within 213/23-1 (Eriboll) are also analogous to volcanic image log facies of lava flows from within the Rosebank Field described by Watton *et al.* (2014, p. 180–182, Fig. 6) and Millett *et al.* (2021, p. 2897, Fig. 9).

Our reinterpretation of 213/23-1 (Eriboll) has proved the presence of T40-T45 lava flows and possible intra- and sub-basaltic plays north of the Rosebank Field, not previously interpreted this far

north (213/23-1 Final Geological Well Report 1999; Passey & Hitchen 2011; Hardman *et al.* 2018). Our results may facilitate further understanding of the true extent and distribution of the intra-basaltic Colsay Member play fairway along the northern Corona Ridge.

Recommendations for future exploration

Many wells along the central-northern Corona Ridge were drilled over 20 years ago (e.g., 213/23-1 Eriboll, 214/09-1 Bunnehaven and 214/04-1 Tobermory, Fig. 1b). Since then, the understanding and subsequent nomenclature of late Paleocene–early Eocene sequences has advanced, which has provided insight into the distribution of Paleogene volcanic rocks (Passey & Hitchen 2011), intra-basaltic lava-field drainage systems (Schofield & Jolley 2013) and lava-field stratigraphy (Passey & Jolley 2009; Hardman *et al.* 2018; Walker *et al.* 2020; Jolley *et al.* 2021).

The results presented in this study emphasise the need for a re-evaluation of wells drilled along the northern Corona Ridge, 214/09-1 (Bunnehaven) and 214/04-1 (Tobermory) (Fig. 1b). Specifically, our results highlight the need for a re-evaluation focused on the possible identification and characterisation of Paleocene-Eocene intra- and sub-basaltic Colsay Member sandstone (sequence T40-T45) plays which may have previously been missed (as we demonstrate within 213/23-1, Eriboll). The reinterpretation of wells, integrated with the knowledge gained from new wells (e.g., Lyon 208/02-1 and Blackrock 204/05b-2, Fig. 1b) and recent publications (e.g. Jolley *et al.* 2021), combined with an appreciation of the complexities of sediment-lava interaction, could not only assist with further location of sequence T40-T45 intra- and sub-basaltic sand fairways but may also facilitate the development of complex reservoirs such as the Rosebank Field. This approach could provide a strategic method to identifying Paleocene–Eocene targets within the under explored gas prone area of the northern FSB, an area which (as of May 2022) holds *c.* 656 bcf of stranded gas as a potential tieback option for any nearby commercial discoveries (post-drill in place volume estimates; Tobermory 464 bcf, 214/04-1 Post-Drill Report 2000; Bunnehaven 192 bcf, 214/09-1 Post-Drill Well Summary Report 2001).

Conclusions

The Faroe-Shetland Basin is one of the only remaining exploration frontiers on the UK Continental Shelf and will also arguably be one of the most important areas to contribute to indigenous oil and gas supply during the next 40 years. Particularly prospective areas of the FSB include the Rona Ridge and Corona Ridge, intra-basinal highs along which the Clair Field (Rona Ridge), Rosebank and Cambo Fields (Corona Ridge) have been discovered. Subsequent exploration and research have largely focussed upon both the Rona Ridge and post-rift Paleocene to Eocene-aged prospectivity along the southern Corona Ridge. Whilst hydrocarbon shows and discoveries prove a working petroleum system is at play within the sub-basins bound by the central-northern Corona Ridge, many aspects of the region's geology are still not fully understood.

Through the interpretation of 3D seismic data integrated with analysis of three exploration wells (213/23-1 Eriboll, 214/21a-2 South Uist and 213/25c-1V North Uist) we have revealed new insights into the structural configuration, geology, and hydrocarbon prospectivity of the central-northern Corona Ridge. We show that:

- The Rosebank intra- and sub-basaltic play concept extends to the NE of the Rosebank Field, along the central-northern Corona Ridge, at least into well 213/23-1 (Eriboll).
- Based on a re-evaluation of available well data we suggest that Triassic strata are absent along the Corona Ridge, challenging previous understanding of Triassic distribution within the central Faroe-Shetland Basin. This interpretation also possibly opens further Devonian–Carboniferous-aged exploration plays of the Clair Group (previously interpreted as Triassic) and the possible presence of gas-prone Carboniferous coals within the northern Faroe-Shetland Basin.
- Using 3D seismic data, we present detailed time–structure maps of the northern-central Corona Ridge. Our results show that the structural configuration of the central-northern Corona Ridge is far more complex than previously understood, including N-S and NNW-SSE-striking faulting oblique to the basinal NE-SW-striking structural trends within the Faroe-Shetland Basin.

Acknowledgements This paper forms part of the lead author's Ph.D. research conducted as part of the Natural Environment Research Council (NERC) Centre for Doctoral Training (CDT) in Oil and Gas at the University of Aberdeen. It is funded by the University of Aberdeen and sponsored by Total E&P UK Limited, whose support is gratefully acknowledged. PGS are thanked for the generous

provision of the FSB MegaSurveyPlus seismic dataset to the Ph.D. project and also for permission to publish part of the dataset (Fig. 3). This paper contains information provided by the North Sea Transition Authority and/or other third parties. Seismic data used throughout this paper were purchased from the UK North Sea Transition Authority (NSTA) National Data Repository (NDR) portal. Well data used throughout this paper are freely available and can be downloaded from the UK NSTA NDR portal. Core photographs were obtained from the BGS Offshore well database. Seismic interpretation was undertaken using Schlumberger Petrel software and well log interpretation was performed using Schlumberger Techlog software, of which academic licenses were kindly provided by Schlumberger and are gratefully acknowledged. Thanks to Conrado Climent, Ole-Petter Hansen, Michael Hertle, Anders Madsen, and Stuart Archer for invaluable discussions during the lead author's time spent working with TotalEnergies in Copenhagen. Thanks also to Christopher Bugg and Matthew Rowlands at TotalEnergies in Aberdeen. Reviewers Tony Doré, Peter Dromgoole and Clayton Grove are thanked for their detailed constructive reviews which improved this manuscript. The views held within this paper do not necessarily represent the views of Schlumberger, TotalEnergies and Ørsted.

Author contributions LKL: conceptualization (lead), data curation (supporting), formal analysis (lead), investigation (lead), methodology (lead), visualization (lead), writing – original draft (lead), writing – review & editing (lead); **NS**: conceptualization (supporting), data curation (supporting), supervision (supporting), visualization (supporting), writing – original draft (supporting), writing – review & editing (supporting); **DWJ**: conceptualization (supporting), data curation (supporting), visualization (supporting), writing – review & editing (supporting); **SPH**: writing – review & editing (supporting); **T-RV**: data curation (supporting), writing – review & editing (supporting); **BK**: visualization (supporting), writing – review & editing (supporting); **DM**: writing – review & editing (supporting); **HC**: writing – review & editing (supporting).

Funding The University of Aberdeen (grant number: RT10121-14), Natural Environment Research Council Centre for Doctoral Training (CDT) in Oil and Gas (grant number: NE/M00578X/1) and Total E&P UK Limited. Principal award-recipient: Lucinda Kate Layfield.

Data Availability The main data that support the findings of this study (Corona 3D, NSTA NDR survey names: TT133D0003 and TT153D0002) are available from the North Sea Transition Authority NDR (https://ndr.nstauthority.co.uk/). Restrictions apply to availability of the PGS FSB MegaSurveyPlus (Fig. 3), which were used under licence for the current study, and so are not publicly available.

References

Abdelmalak, M.M., Faleide, J.I., Planke, S., Gernigon, L., Zastrozhnov, D., Shephard, G.E. and Myklebust, R. 2017. The T-Reflection and the Deep Crustal Structure of the Vøring Margin, Offshore mid-Norway. *Tectonics,* **36**, 2497–2523, https://doi.org/10.1002/2017TC004617

Austin, J.A., Cannon, S.J.C. and Ellis, D. 2014. Hydrocarbon exploration and exploitation West of Shetlands. *In:* Cannon, S.J.C and Ellis, D. (eds) *Hydrocarbon Exploration to Exploitation West of Shetlands.* Geological Society of London Special Publication, **397**, 1–10, https://doi.org/10.1144/SP397.13

Barr, D., Savory, K.E, Fowler, S.R., Arman, K. & McGarrity, J.P. 2007. Pre-development fracture modelling in the Clair field, west of Shetland. *In:* Lonergan, L., Jolly, R.J.H., Rawnsley, K. and Sanderson, D.J. (eds) *Fractured Reservoirs.* Geological Society of London Special Publication, **270**, 205–225, https://doi.org/10.1144/GSL.SP.2007.270.01.14

Bell, B.R. and Jolley, D.W. 1997. Application of palynological data to the chronology of the Palaeogene lava fields of the British Province: implications for magmatic stratigraphy. *Journal of the Geological Society*, **154**, 701–708, https://doi.org/10.1144/gsjgs.154.4.0701

Bonter, D.A. and Trice, R. 2019. An integrated approach for fractured basement characterization: the Lancaster Field, a case study in the UK. *Petroleum Geoscience,* **25**, 400–414, https://doi.org/10.1144/petgeo2018-152

BP Exploration Operating Company Limited (BP) 2013. 213/25c-1V (North Uist) Composite Log. North Sea Transition Authority UK National Data Repository, https://ndr.nstauthority.co.uk/

BP Exploration Operating Company Limited (BP) 2013. End of Well Report, 213/25c-1, 1Z, 1Y, 1X, 1W, 1V. North Sea Transition Authority UK National Data Repository, https://ndr.nstauthority.co.uk/

BP Exploration Operating Company Limited (BP) 2013. North Uist Exploration Well, 213/25c-1, 1Z, 1Y, 1X, 1W, 1V, Geological Operations Report. North Sea Transition Authority UK National Data Repository, https://ndr.nstauthority.co.uk/

British Geological Survey (BGS) 1996. *Tectonic Map of Britain, Ireland and adjacent areas (1:500,000).* Pharaoh, T.C., Morris, J.H., Long, C.B. and Ryan, P.D. (compilers). British Geological Survey, Nottingham, https://largeimages.bgs.ac.uk/iip/mapsportal.html?id=1004599

British Geological Survey (BGS) 2021. *Offshore Hydrocarbon Wells,* webapps.bgs.ac.uk/data/offshoreWells

Chevron Upstream Europe 2007. Rosebank / Lochnagar Appraisal Well. Well 213/27-2. Geological end of well report & lessons learned. North Sea Transition Authority UK National Data Repository, https://ndr.nstauthority.co.uk/

ChevronTexaco Upstream Europe 2004. Rosebank-Lochnagar Exploration Well. 213/27-1 & 1Z End of Well Report. Geological end of well report & lessons learned. North Sea Transition Authority UK National Data Repository, https://ndr.nstauthority.co.uk/

Chevron Upstream Europe 2009. 213/27-3 & 3Z. Rosebank-Lochnagar Exploration Well. Geological & Geophysical End of Well Report. North Sea Transition Authority UK National Data Repository, https://ndr.nstauthority.co.uk/

Clark, J., Mazzuchelli, D., Rowlands, M., Jebara, N. and Parry, C. 2020. The Edradour Field, Block 206/4a, UK Atlantic Margin. *In:* Goffey, G. and Gluyas, J. G. (eds) *United Kingdom Oil and Gas Fields: 50th Anniversary Commemorative Volume.* Geological Society, London, Memoirs, **52**, 952–957, https://doi.org/10.1144/M52-2018-23

CNOOC Limited 2017. License P.1192 Relinquishment Report. North Sea Transition Authority UK National Data Repository, https://ndr.nstauthority.co.uk/

Cohen, K.M., Finney, S.C., Gibbard, P.L. and Fan, J.-X. 2013. The ICS International Chronostratigraphic Chart. *Episodes,* **36**(3), 199–204, https://doi.org/10.18814/epiiugs/2013/v36i3/002

Conoco (UK) Limited 1996. 206/5-2 Final Geological Report. North Sea Transition Authority UK National Data Repository, https://ndr.nstauthority.co.uk/

Coward, M.P. 1990. Caledonian and Variscan framework to NW Europe. *In*: Hardman, R.P.F. and Brooks, J. (eds) *Tectonic Events Responsible for Britain's Oil and Gas Reserves*. Geological Society of London Special Publication, **55,** 1–34, https://doi.org/10.1144/GSL.SP.1990.055.01.01

Dean, K., McLachlan, K. and Chambers, A. 1999. Rifting and the development of the Faroe-Shetland Basin. *In:* Fleet, A.J. and Boldy, S.A.R. (eds) *Petroleum Geology of Northwest Europe: Proceedings of the 5th Conference.* Geological Society, London, 947–956, https://doi.org/10.1144/0050533

Doré, A.G., Lundin, E.R., Fichler, C. and Olesen, O. 1997. Patterns of basement structure and reactivation along the NE Atlantic margin. *Journal of the Geological Society*, **154**, 85–92, https://doi.org/10.1144/gsjgs.154.1.0085

Doré, A.G., Lundin E.R., Jensen, L.N., Birkeland, Ø., Eliassen, P.E. and Fichler, C. 1999. Principal tectonic events in the evolution of the northwest European Atlantic margin. *In:* Fleet, A.J. and

Boldy, S.A.R. (eds) *Petroleum Geology of Northwest Europe: Proceedings of the 5th Conference.* Geological Society, London, 41–61, https://doi.org/10.1144/0050041

Doré, A.G., Lundin, E.R., Kusznir, N.J. and Pascal, C. 2008. Potential mechanisms for the genesis of Cenozoic domal structures on the NE Atlantic margin: pros, cons and some new ideas. *In:* Johnson, H., Doré, A.G., Gatliff, R.W., Holdsworth, R.W., Lundin, E. and Ritchie, J.D. (eds) *The Nature of Compression in Passive Margins.* Geological Society of London Special Publication, **306**, 1–26, https://sp.lyellcollection.org/content/306/1/1

Duncan, L., Helland-Hansen, D. and Dennehy, C. 2009. The Rosebank Discovery, A new play type in intra basalt reservoirs of the North Atlantic volcanic province. In: 6th European Production and Development Conference and Exhibition (DEVEX), Abstracts. Chevron Upstream Europe, 13 May, Aberdeen, http://docplayer.net/40657397-The-rosebank-discovery-a-new-play-type-in-intra-basalt-reservoirs-of-the-north-atlantic-volcanic-province-devex-aecc-13-may-2009.html

Duncan, L.J., Dennehy, C.J., Ablard, P.M. and Wallis, D.W. 2020. The Rosebank Field, Blocks 213/27a, 213/26b, 205/1a and 205/2a, UK Atlantic Margin. *In:* Goffey, G. and Gluyas, J.G. (eds) *United Kingdom Oil and Gas Fields: 50th Anniversary Commemorative Volume*. Geological Society, London, Memoirs, **52**, 980–989, https://doi.org/10.1144/M52-2018-42

Ebdon, C.C., Granger, P.J., Johnson, H.D. and Evans, A.M. 1995. Early Tertiary evolution and stratigraphy of the Faeroe-Shetland Basin: implications for hydrocarbon prospectivity. *In:* Scrutton, R.A., Stoker, M.S., Shimmield, G.B. and Tudlope, A.W. (eds) *The Tectonics, Sedimentation and Palaeoceanography of the North Atlantic Region.* Geological Society of London Special Publication, **90**, 51–69, https://doi.org/10.1144/GSL.SP.1995.090.01.03

Ellis, D. and Stoker, M.S. 2014. The Faroe-Shetland Basin: A regional perspective from the Paleocene to the present day and its relationship to the opening of the North Atlantic Ocean. *In:* Cannon, S.J.C and Ellis, D. (eds) *Hydrocarbon Exploration to Exploitation West of Shetlands.* Geological Society of London Special Publication, **397**, 11–31, https://doi.org/10.1144/SP397.1

Ellis, D., Passey, S.R., Jolley, D.W. and Bell, B.R. 2009. Transfer zones: the application of new geological information from the Faroe Islands applied to the offshore exploration of intra and sub-basalt strata. *In:* Ziska, H. and Varming, T. (eds) *Faroe Islands Exploration Conference: Proceedings of the 2nd Conference.* Faroese Society of Sciences and Humanities, Tórshavn, 205–226.

Energy Voice 2012. Oil & Gas: North Uist's price tag to exceed £100m, https://www.energyvoice.com/oilandgas/29442/north-uists-price-tag-to-exceed-100m/

ExxonMobil 2000. Well 214/04-1, Post-Drill Report. North Sea Transition Authority UK National Data Repository, https://ndr.nstauthority.co.uk/

ExxonMobil 2001. Post-Drill Well Summary Report, Well 214/09-1, Tranche 61. North Sea Transition Authority UK National Data Repository, https://ndr.nstauthority.co.uk/

Fletcher, R., Kusznir, K., Roberts, A. and Hunsdale, R. 2013. The formation of a failed continental breakup basin: The Cenozoic development of the Faroe-Shetland Basin. *Basin Research*, **25**, 1–22, https://doi.org/10.1111/bre.12015

Funck, T., Geissler, W.H., Kimbell, G.S., Gradmann, S., Erlendsson, Ö., McDermott, K. and Petersen, U.K. 2017. Moho and basement depth in the NE Atlantic Ocean based on seismic refraction data and receiver functions. *In:* Péron-Pinvidic, G., Hopper, J.R., Stoker, M.S., Gaina, C., Doornenbal, J.C., Funck, T. and Árting, U.E. (eds) *The NE Atlantic Region: A Reappraisal of Crustal Structure, Tectonostratigraphy and Magmatic Evolution.* Geological Society of London Special Publication, **447**, 207–231, https://doi.org/10.1144/SP447.1

Gardiner, D., Schofield, N., Finlay, A., Mark, N., Holt, L., Grove, C., Forster, C. and Moore, J. 2019. Modeling petroleum expulsion in sedimentary basins: The importance of igneous intrusion timing and basement composition. *Geology,* **47**, 904–908, https://doi.org/10.1130/G46578.1

Goodchild, M.W., Henry, K.L., Hinkley, R.J. and Imbus, S.W. 1999. The Victory gas field, West of Shetland. *In:* Fleet, J. and Boldy, S.A.R. (eds) *Petroleum Geology of Northwest Europe: Proceedings of the 5th Conference.* Geological Society, London, 713–724, https://doi.org/10.1144/0050713

Hardman, J., Schofield, N., Jolley, D., Hartley, A., Holford, S. and Watson, D. 2018. Controls on the distribution of volcanism and intra-basaltic sediments in the Cambo-Rosebank region, West of Shetland. *Petroleum Geoscience*, **25**, 71–89, https://doi.org/10.1144/petgeo2017-061

Hardwick, A., Travis, T., Stokes, S. and Hart, M. 2010. Lows and highs: using low frequencies and improved velocity tools to image complex ridges and basement highs in the Faroe- Shetland Basin. *First Break,* **28**, 61–67, https://doi.org/10.3997/1365-2397.28.9.41392

Haq, B.U., Hardenbol, J. and Vail, P.R. 1987. Chronology of Fluctuating Sea Levels since the Triassic. *Science,* **235**, 1156–1167, https://doi.org/10.1126/science.235.4793.1156

Herries, R., Poddubiuk, R. and Wilcockson, P. 1999. Solan, Strathmore and the back basin play, West of Shetland. *In:* Fleet, J. and Boldy, S.A.R. (eds) *Petroleum Geology of Northwest Europe: Proceedings of the 5th Conference.* Geological Society, London, 693–712, https://doi.org/10.1144/0050693

Hitchen, K. and Ritchie, J.D. 1987. Geological review of the West Shetland area. *In:* Brooks, J. and Glennie, K.W. (eds) *Petroleum Geology of North West Europe.* Graham & Trotman, London, 737–749.

Holdsworth, R.E, Morton, A., Frei, D., Gerdes, A., Strachan, R.A., Dempsey, E., Warren, C. and Whitham, A. 2019. The nature and significance of the Faroe-Shetland Terrace: Linking Archaean basement blocks across the North Atlantic. *Precambrian Research,* **321**, 154–171, https://doi.org/10.1016/j.precamres.2018.12.004

Holford, S.P., Tassone, D.R., Stoker, M.S. and Hillis, R.R. 2015. Contemporary stress orientations in the Faroe-Shetland region. *Journal of the Geological Society*, **173**, 142–152, https://doi.org/10.1144/jgs2015-048

Hughes, S., Barton, P.J. and Harrison, D.J. 1997. Characterizing the Mid-Faeroe Ridge using seismic velocity measurements. *Papers on Geomagnetism and Paleomagnetism Marine Geology and Geophysics*, **102**, 7837–7847, https://doi.org/10.1029/96JB03809

Iliffe, J.E., Robertson, A.G., Ward, G.H.F., Wynn, C., Pead, S.D.M., and Cameron, M. 1999. The importance of fluid pressures and migration to the hydrocarbon prospectivity of the Faeroe-Shetland White Zone. *In:* Fleet, A.J., and Boldy, S.A.R. (eds) *Petroleum Geology of Northwest Europe – Proceedings of the 5th Conference.* Geological Society, London, 601–611, https://doi.org/10.1144/0050601

Jolley, D.W. and Bell, B.R. 2002. The evolution of the North Atlantic Igneous Province and the opening of the NE Atlantic rift. *In:* Jolley, D.W. and Bell, B.R. (eds) *The North Atlantic Igneous Province: Stratigraphy, Tectonic, Volcanic and Magmatic Processes.* Geological Society of London Special Publication, **197**, 1–13, https://doi.org/10.1144/GSL.SP.2002.197.01.01

Jolley, D.W., Millett, J.M., Schofield, N., Broadley, L. & Hole, M.J. 2021. Stratigraphy of volcanic rock successions of the North Atlantic rifted margin: the offshore record of the Faroe Shetland and Rockall basins. *Earth and Environmental Science Transactions of the Royal Society of Edinburgh,* 1–28. First published online 26 May 2021, https://doi.org/10.1017/S1755691021000037

Joseph, S., Lu, X., Bykov, K. and Douillard, A. 2017. Extensive Broadband 3D Seismic to De-risk and Mature the West of Shetland Exploration Portfolio. 79th EAGE Conference & Exhibition, 12-15 June, Paris, https://www.earthdoc.org/content/papers/10.3997/2214-4609.201700816

Kinny, P.D., Friend, C.R.L., and Love, G.J. 2005. Proposal for a terrane-based nomenclature for the Lewisian Gneiss Complex of NW Scotland. *Journal of the Geological Society,* **162**, 175–186.

Knott, S.D., Burchell, M.T., Jolley, E.J. and Fraser, A.J. 1993. Mesozoic to Cenozoic plate reconstructions of the North Atlantic and hydrocarbon plays of the Atlantic margins. *In:* Parker, J.R. (ed.) *Petroleum Geology of Northwest Europe: Proceedings of the 4th Conference.* Geological Society, London, 953–974, https://doi.org/10.1144/0040953

Lamers, E. and Carmichael, S.M.M. 1999. The Paleocene deep-water sandstone play west of Shetland. *In:* Fleet, J. and Boldy, S.A.R. (eds) *Petroleum Geology of Northwest Europe: Proceedings of the 5th Conference.* Geological Society, London, 645–659, https://doi.org/10.1144/0050645

Larsen, M., Rasmussen, T. and Hjelm, L. 2010. Cretaceous revisited: exploring the syn-rift play of the Faroe-Shetland Basin. *In:* Vining, B.A. and Pickering, S.C. (eds) *Petroleum Geology: From Mature Basins to New Frontiers – Proceedings of the 7th Petroleum Geology Conference.* Geological Society, London, 953–962, https://doi.org/10.1144/0070953

Makris, J., Papoulia, I. and Ziska, H. 2009. Crustal structure of the Shetland – Faeroe Basin from long offset seismic data. *In:* Ziska, H. and Varming, T. (eds) *Faroe Islands Exploration Conference: Proceedings of the 2nd Conference.* Faroese Society of Sciences and Humanities, Tórshavn, 30–42.

Mark, N.J., Schofield, N., Gardiner, D., Holt, L., Grove, C., Watson, D., Alexander, A. and Poore, H. 2018a. Overthickening of sedimentary sequences by igneous intrusions. *Journal of the Geological Society,* **176**, 46–60, https://doi.org/10.1144/jgs2018-112

Mark, N. J., Schofield, N., Pugliese, S., Watson, D., Holford, S., Muirhead, D., Brown, R. and Healy, D. 2018b. Igneous intrusions in the Faroe Shetland basin and their implications for hydrocarbon exploration; new insights from well and seismic data. *Marine and Petroleum Geology* (2018), **92**, 733–753, https://doi.org/10.1016/j.marpetgeo.2017.12.005

Millett, J.M., Jerram, D.A., Manton, B., Planke, S., Ablard, P., Wallis, D., Hole, M.J., Brandsen, H., Jolley, D.W. and Dennehy, C. 2021. The Rosebank Field, NE Atlantic: Volcanic characterisation of an inter-lava hydrocarbon discovery. *Basin Research,* **33(6)**, 2883–2913, https://doi.org/10.1111/bre.12585

Mobil North Sea Limited 1998. 213/23-1 Composite Well Log. North Sea Transition Authority UK National Data Repository, https://ndr.nstauthority.co.uk/

Mobil North Sea Limited 1999. Final Geological Well Report 213/23-1 Eriboll. North Sea Transition Authority UK National Data Repository, https://ndr.nstauthority.co.uk/

Mobil North Sea Limited 1999. Well: 213/23-1, Biostratigraphy of the Intervals 4398'-6168' and 6650'-14200'. North Sea Transition Authority UK National Data Repository, https://ndr.nstauthority.co.uk/

Mobil North Sea Limited 1999. Sedimentology and Petrography of Well 213/23-1. Report No. 24/98. Compiled by Leppard Sedimentology & Petroclays. North Sea Transition Authority UK National Data Repository, https://ndr.nstauthority.co.uk/

Morton, A. and Milne, A. 2012. Heavy mineral stratigraphic analysis on the Clair Field, UK, west of Shetlands: a unique real-time solution for red-bed correlation while drilling. *Petroleum Geoscience,* **18**, 115–128, https://doi.org/10.1144/1354-079311-026

Morton, A., Hallsworth, C., Kunka, J., Laws, E., Payne, S. and Walder, D. 2010. Heavy-mineral stratigraphy of the Clair Group (Devonian-Carboniferous) in the Clair Field, West of Shetland, U.K. *In:* Ratcliffe, K.T. and Zaitlin, B.A. (eds) *Application of Modern Stratigraphy Techniques: Theory and Case Histories.* SEPM Special Publication, London, **94**, 183–199, https://doi.org/10.2110/sepmsp.094.183

Moy, D.J. and Imber, J. 2009. A critical analysis of the structure and tectonic significance of rift-oblique lineaments ('transfer zones') in the Mesozoic-Cenozoic succession of the Faroe-

Shetland Basin, NE Atlantic margin. *Journal of the Geological Society*, **166**, 831–844, https://doi.org/10.1144/0016-76492009-010

Mudge, D.C. and Rashid, B. 1987. The geology of the Faeroe Basin area. *In:* Brooks, J. and Glennie, K.W. (eds) *Petroleum Geology of North West Europe.* Graham & Trotman, London, 751–763.

Nelson, C.E., Jerram, D.A., and Hobbs, R.W. 2009. Flood basalt facies from borehole data: Implications for prospectivity and volcanology in volcanic rifted margins. *Petroleum Geoscience,* **15(4)**, 313–324, https://doi.org/10.1144/1354-079309-842

Nichols, G.J. 2005. Sedimentary evolution of the lower Clair Group, Devonian, West of Shetland: climate and sediment supply controls on fluvial, aeolian and lacustrine deposition. *In:* Doré, A.G. and Vining, B.A. (eds) *Petroleum Geology: North-West Europe and Global Perspectives—Proceedings of the 6th Petroleum Geology Conference*. Geological Society, London, 957–967, https://doi.org/10.1144/0060957

North Sea Transition Authority (NSTA) 2019. UK Oil and Gas: Reserves and Resources, https://www.nstauthority.co.uk/data-centre/data-downloads-and-publications/reserves-and-resources/

North Sea Transition Authority (NSTA) 2021. OGA Overview 2021, https://www.nstauthority.co.uk/news-publications/publications/2021/oga-overview-2021/

North Sea Transition Authority (NSTA) 2022. *UK National Data Repository,* https://ndr.nstauthority.co.uk/

Ogilvie, S., Barr, D., Roylance, P. and Dorling, M. 2015. Structural geology and well planning in the Clair Field. *In:* Richards, F.L., Richardson, N.J., Rippington, S.J., Wilson, R.W. and Bond, C.E. (eds) *Industrial Structural Geology: Principles, Techniques and Integration.* Geological Society of London Special Publication, **421**, 197–212, https://doi.org/10.1144/SP421.7

OMV 2015. Relinquishment report for Licence P1997. North Sea Transition Authority UK National Data Repository, https://ndr.nstauthority.co.uk/

Passey, S. and Hitchen, K. 2011. 9 Cenozoic (igneous). *In:* Ritchie, J.D., Ziska, H., Johnson, H. and Evans, D. (eds) *Geology of the Faroe-Shetland Basin and Adjacent Areas*. British Geological Survey, Nottingham, UK, https://pubs.bgs.ac.uk/publications.html?pubID=B06836

Passey, S. and Jolley, D.W. 2009. A revised lithostratigraphic nomenclature for the Palaeogene Faroe Islands Basalt Group, NE Atlantic Ocean. *Earth and Environmental Science Transactions of the Royal Society of Edinburgh*, **99**, 127–158, https://doi.org/10.1017/S1755691009008044

Petersen, U.K. and Funck, T. 2017. Review of velocity models in the Faroe-Shetland Channel. *In:* Péron-Pinvidic, G., Hopper, J.R., Stoker, M.S., Gaina, C., Doornenbal, J.C., Funck, T. and Árting, U.E. (eds) *The NE Atlantic Region: A Reappraisal of Crustal Structure, Tectonostratigraphy and Magmatic Evolution*. Geological Society of London Special Publication, **447**, 357–374, https://doi.org/10.1144/SP447.7

Poppitt, S., Duncan, L.J., Preu, B., Fazzari, F. and Archer, J. 2018. The influence of volcanic rocks on the characterization of Rosebank Field – new insights from ocean-bottom seismic data and geological analogues integrated through interpretation and modelling. *In:* Bowman, M. and Levell, B. (eds) *Petroleum Geology of NW Europe: 50 Years of Learning – Proceedings of the 8th Petroleum Geology Conference*. Geological Society, London 373–384, https://doi.org/10.1144/PGC8.6

Quinn, M. and Ziska, H. 2011. 5 Permian and Triassic. *In:* Ritchie, J.D., Ziska, H., Johnson, H. and Evans, D. (eds) *Geology of the Faroe-Shetland Basin and Adjacent Areas.* British Geological Survey, Nottingham, UK, https://pubs.bgs.ac.uk/publications.html?pubID=B06836

Quinn, M., Varming, T. and Ólavsdottir, J. 2011. 12 Petroleum Geology. *In:* Ritchie, J.D., Ziska, H., Johnson, H. and Evans, D. (eds) *Geology of the Faroe-Shetland Basin and Adjacent Areas.* British Geological Survey, Nottingham, UK, https://pubs.bgs.ac.uk/publications.html?pubID=B06836

Ridd, M.F. 1981. Petroleum geology west of the Shetlands. *In:* L.V. Illing and G.D. Hobson (eds) *Petroleum Geology of the Continental Shelf of North-West Europe*. Heyden, London, 414–425.

Ridd, M.F. 1983. Aspects of the Tertiary geology of the Faroe-Shetland Channel. *In:* Bott, M.H.P., Saxov, S., Talwani, M. and Thiede, J. (eds) *Structure and development of the Greenland –Scotland Ridge: new methods and concept.* Plenum Press, New York, 91–108.

Rippington, S., Mazur, S. and Warner, J. 2015. The crustal architecture of the Faroe-Shetland Basin: insights from a newly merged gravity and magnetic dataset. *In:* Richards, F.L., Richardson, N.J., Rippington, S.J., Wilson, R.W. and Bond, C.E. (eds) *Industrial Structural Geology: Principles, Techniques and Integration.* Geological Society of London Special Publication, **421**, 169–196, https://doi.org/10.1144/SP421.10

Ritchie, J.D. and Varming, T. 2011. 6 Jurassic. *In:* Ritchie, J.D., Ziska, H., Johnson, H. and Evans, D. (eds) *Geology of the Faroe-Shetland Basin and Adjacent Areas.* British Geological Survey, Nottingham, UK, https://pubs.bgs.ac.uk/publications.html?pubID=B06836

Ritchie, J.D., Johnson, H., Quinn, M.F. and Gatliff, R.W. 2008. The effects of Cenozoic compression within the Faroe-Shetland Basin and adjacent areas. *In:* Johnson, H., Doré, A.G., Gatliff, R.W., Holdsworth, R.W., Lundin, E. and Ritchie, J.D. (eds) *The Nature of Compression in Passive Margins.* Geological Society of London Special Publication, **306**, 121–136, https://doi.org/10.1144/SP306.5

Ritchie, J.D., Ziska, H., Kimbell, G., Quinn, M. and Chadwick, A. 2011. 2 Structure. *In:* Ritchie, J. D., Ziska, H., Johnson, H. and Evans, D. (eds) *Geology of the Faroe-Shetland Basin and Adjacent Areas.* British Geological Survey, Nottingham, UK, https://pubs.bgs.ac.uk/publications.html?pubID=B06836

Roberts, D.G., Thompson, M., Mitchener, B., Hossack, J., Carmichael, S. and Bjørnseth, H.M. 1999. Palaeozoic to Tertiary rift and basin dynamics: mid-Norway to the Bay of Biscay – a new context for hydrocarbon prospectivity in the deep water frontier. *In:* Fleet, A.J. and Boldy, S.A.R. (eds) *Petroleum Geology of Northwest Europe: Proceedings of the 5th Conference.* Geological Society, London, 7–40, https://doi.org/10.1144/0050007

Roberts, A.W. White, R.S. and Christie, P.A.F. 2009. Imaging igneous rocks on the North Atlantic rifted continental margin. *Geophysical Journal International,* **179**, 1024–1038, https://doi.org/10.1111/j.1365-246X.2009.04306.x

Robertson, A.G., Ball, M., Costaschuk, J., Davidson, J., Guliyev, N., Kennedy, B., Leighton, C., Nash, T. and Nicholson, H. 2020. The Clair Field, Blocks 206/7a, 206/8, 206/9a, 206/12a and 206/13a, UK Atlantic Margin. *In:* Goffey, G. and Gluyas, J.G. (eds) *United Kingdom Oil and Gas Fields: 50th Anniversary Commemorative Volume.* Geological Society, London, Memoirs, **52**, 980–989, https://doi.org/10.1144/M52-2018-76

Rogers, S.F. 2003. Critical stress-related permeability in fractured rocks. *In:* Ameen, M. (ed.) *Fracture and In-Situ Stress Characterization of Hydrocarbon Reservoirs.* Geological Society of London Special Publication, **209**, 7–16, https://doi.org/10.1144/GSL.SP.2003.209.01.02

Rumph, B., Reaves, C.M., Orange, V.G. and Robinson, D.L. 1993. Structuring and transfer zones in the Faroe Basin in a regional tectonic context. *In:* Parker, J.R. (ed) *Petroleum geology of northwest Europe: Proceedings of the 4th conference.* Geological Society, London, 999–1009, https://doi.org/10.1144/0040999

Schiffer, C., Doré, A.G., Foulger, G.R., Franke, D., Geoffroy, L., Gernigon, L., Holdsworth, B., Kusznir, N., Lundin, E., McCaffrey, K., Peace, A.L., Petersen, K.D., Phillips, T.B., Stephensen, R.,

Stoker, M and Welford, J.K. 2020. Structural inheritance in the North Atlantic. *Earth-Science Reviews,* **206**, 102975, https://doi.org/10.1016/j.earscirev.2019.102975

Schöpfer, K. and Hinsch, R. 2019. Late Palaeozoic – Mesozoic tectonostratigraphic development of the eastern Faroe-Shetland Basin: New insights from high-resolution 3D seismic and well data. *Marine and Petroleum Geology*, **109**, 494–518, https://doi.org/10.1016/j.marpetgeo.2019.04.007

Schofield, N. and Jolley, D.W. 2013. Development of intra-basaltic lava-field drainage systems within the Faroe-Shetland Basin. *Petroleum Geoscience,* **19**, 273–288, https://doi.org/10.1144/petgeo2012-061

Schofield, N., Holford, S., Millett, J., Brown, D., Jolley, D., Passey, S.R., Muirhead, D., Grove, C., Magee, C., Murray, J. and Hole, M. 2017. Regional magma plumbing and emplacement mechanisms of the Faroe-Shetland Sill Complex: implications for magma transport and petroleum systems within sedimentary basins. *Basin Research*, **29**, 41–63, https://doi.org/10.1111/bre.12164

Schofield, N., Holford, S., Edwards, A., Mark, N., Pugliese., S. 2020. Overpressure transmission through interconnected igneous intrusions. *AAPG Bulletin,* **104**, 285–303, https://doi.org/10.1306/05091918193

Scotchman, I.C., Griffith, C.E., Holmes, A.J. and Jones, D.M. 1998. The Jurassic petroleum system north and west of Britain: a geochemical oil-source correlation study. *Organic Geochemistry*, **29**, 671–700, https://doi.org/10.1016/S0146-6380(98)00183-1

Scotchman, I.C., Carr, A.D. and Parnell, J. 2006. Hydrocarbon generation modelling in a multiple rifted and volcanic basin: a case study in the Foinaven Sub-basin, Faroe-Shetland Basin, UK Atlantic margin. *Scottish Journal of Geology*, **42**, 1–19, https://doi.org/10.1144/sjg42010001

Scotchman I.C., Doré A.G. and Spencer, A.M. 2016. Petroleum systems and results of exploration on the Atlantic margins of the UK, Faroes & Ireland: what have we learnt? *In:* Bowman M. and Levell B. (eds) *Petroleum Geology of NW Europe: 50 Years of Learning – Proceedings of the 8th Petroleum Geology Conference.* Geological Society, London, 187–197, https://doi.org/10.1144/PGC8.14

Shell U.K. Limited 2010. South Uist 214/21a-2 End of Well Report. North Sea Transition Authority UK National Data Repository, https://ndr.nstauthority.co.uk/

Shell U.K. Limited 2014. Relinquishment Report for License P.799 Relinquishment of Block 214/21a. North Sea Transition Authority UK National Data Repository, https://ndr.nstauthority.co.uk/

Sheriff, R.E. and Geldart, L.P. 1982. *Exploration Seismology.* Cambridge University Press, Cambridge, UK.

Siccar Point Energy 2020a. Corona Ridge Area, siccarpointenergy.co.uk/our-portfolio/corona-ridge-area

Siccar Point Energy 2020b. Siccar Point Energy Announces Cambo FID Deferral to 2021, siccarpointenergy.co.uk/uploads/20200330_Cambo_FID_FINAL.pdf

Siccar Point Energy 2020c. Geological Operations End of Well Report 208/02-1 (Lyon). North Sea Transition Authority UK National Data Repository, https://ndr.nstauthority.co.uk/

Smallwood, J.R. 2004. Tertiary inversion in the Faroe-Shetland Channel and the development of major erosional scarps. *In:* Davies, R.J., Cartwright, J., Stewart, S.A., Lappin, M. and Underhill, J.R. (eds) *3D Seismic Technology: Application to the Exploration of Sedimentary Basins.* Geological Society, London, Memoirs, **29**, 187–198, https://doi.org/10.1144/GSL.MEM.2004.029.01.18

Smallwood, J.R. and Gill, C.E. 2002. The rise and fall of the Faroe-Shetland Basin: evidence from seismic mapping of the Balder Formation. *Journal of the Geological Society*, **159**, 627–630, https://doi.org/10.1144/0016-764902-064

Smallwood, J.R. and Maresh, J. 2002. The properties, morphology and distribution of igneous sills: modelling, borehole data and 3D seismic data from the Faeroe-Shetland area. *In:* Jolley, D.W. and Bell, B.R. (eds) *The North Atlantic Igneous Province: Stratigraphy, Tectonic, Volcanic and Magmatic Processes.* Geological Society of London Special Publication, **197**, 271–306, https://doi.org/10.1144/GSL.SP.2002.197.01.11

Smallwood, J.R. and Kirk, W.J. 2005. Paleocene exploration in the Faroe-Shetland Channel: disappointments and discoveries. *In:* Doré, A.G. and Vining, B.A. (eds) *Petroleum Geology: North-West Europe and Global Perspectives – Proceedings of the 6th Petroleum Geology Conference.* Geological Society, London, 977–991, https://doi.org/10.1144/0060977

Smith, K. and Ziska, H. 2011. 4. Devonian and Carboniferous. *In:* Ritchie, J. D., Ziska, H., Johnson, H. and Evans, D. (eds) *Geology of the Faroe-Shetland Basin and Adjacent Areas*. British Geological Survey, Nottingham, UK, https://pubs.bgs.ac.uk/publications.html?pubID=B06836

Sørensen, A.B. 2003. Cenozoic basin development and stratigraphy of the Faroes area. *Petroleum Geoscience*, **9**, 189–207, https://doi.org/10.1144/1354-079302-508

Stoker, M.S. 2016. Cretaceous tectonostratigraphy of the Faroe-Shetland region. *Scottish Journal of Geology,* **52**, 19–41, https://doi.org/10.1144/sjg2016-004

Stoker, M.S. and Varming, T. 2011. 8 Cenozoic (sedimentary). *In:* Ritchie, J.D., Ziska, H., Johnson, H. and Evans, D. (eds) *Geology of the Faroe-Shetland Basin and Adjacent Areas.* British Geological Survey, Nottingham, UK, https://pubs.bgs.ac.uk/publications.html?pubID=B06836

Stoker, M.S. and Ziska, H. 2011. 7 Cretaceous. *In:* Ritchie, J.D., Ziska, H., Johnson, H. and Evans, D. (eds) *Geology of the Faroe-Shetland Basin and Adjacent Areas.* British Geological Survey, Nottingham, UK, https://pubs.bgs.ac.uk/publications.html?pubID=B06836

Stoker, M.S., Hitchen, K. and Graham, C.C. 1993. *United Kingdom Offshore Regional Report: The Geology of the Hebrides and West Shetland shelves, and adjacent deep-water areas.* HMSO for the British Geological Survey, London, https://pubs.bgs.ac.uk/publications.html?pubID=B01843

Stoker, M., Smith, K., Varming, T., Johnson, H., Olavsdottir, J. 2012. *Eocene (Stronsay Group) post-rift stratigraphy of the Faroe-Shetland region.* British Geological Survey, Edinburgh, UK, http://nora.nerc.ac.uk/id/eprint/530667/1/CR12009N.pdf

Stoker, M., Doornenbal, H., Hopper, J.R. and Gaina, C. 2014. Chapter 7: Tectonostratigraphy. *In:* Hopper, J.R., Funck, T., Stoker, M., Árting, U., Peron-Pinvidic, G. Doornenbal, H. and Gaina, C. (eds) *Tectonostratigraphic Atlas of the North-East Atlantic Region.* Geological Survey of Denmark and Greenland, Copenhagen, Denmark.

Stoker, M.S., Holford, S.P. and Hillis, R.R. 2017a. A rift-to-drift record of vertical crustal motions in the Faroe-Shetland Basin, NW European margin: establishing constraints on NE Atlantic evolution. *Journal of the Geological Society,* **175**, 263–274, https://doi.org/10.1144/jgs2017-076

Stoker, M.S., Stewart, M.A., Shannon, P.M., Bjerager, M., Nielsen, T., Blischke, A., Hjelstuen, B.O., Gaina, C., McDermott, K. and Ólavsdóttir, J. 2017b. An overview of the Upper Palaeozoic-Mesozoic stratigraphy of the NE Atlantic region. *In:* Péron-Pinvidic, G., Hopper, J.R., Stoker, M.S., Gaina, C., Doornenbal, J.C., Funck, T. and Árting, U.E. (eds) *The NE Atlantic Region: A Reappraisal of Crustal Structure, Tectonostratigraphy and Magmatic Evolution.* Geological Society of London Special Publication, **447**, 11–68, https://doi.org/10.1144/SP447.2

Swiecicki, T., Wilcockson, P., Canham, A., Whelan, G. and Homann, H. 1995. Dating, correlation and stratigraphy of the Triassic sediments in the West Shetlands area. *In:* Boldy, S.A.R. (ed.) 1995. *Permian and Triassic Rifting in Northwest Europe.* Geological Society of London Special Publication, **91**, 57–85, https://doi.org/10.1144/GSL.SP.1995.091.01.04

Tassone, D.R., Holford, S.P., King, R., Tingay, M.R.P. and Hillis, R. 2017. Contemporary stress and neotectonics in the Otway Basin, southeastern Australia. *In:* Turner, J.P., Healy, D., Hillis, R.R.

and Welch, M.J. (eds) *Geomechanics and Geology*. Geological Society of London Special Publication, **458**, 49–88, https://doi.org/10.1144/SP458.10

The Expro Group 1999. 213/23-1 Well Site Test Report. North Sea Transition Authority UK National Data Repository, https://ndr.nstauthority.co.uk/

Trice, R. 2014. Basement exploration, West of Shetlands: progress in opening a new play on the UKCS. *In:* Cannon, S.J.C and Ellis, D. (eds) *Hydrocarbon Exploration to Exploitation West of Shetlands.* Geological Society of London Special Publication, **397**, 81–105, https://doi.org/10.1144/SP397.3

Underhill, J.R. 2003. The tectonic and stratigraphic framework of the United Kingdom's oil and gas fields. *In:* Gluyas, J.G. and Hichens, H.M. (eds) *United Kingdom Oil and Gas Fields Commemorative Millennium Volume.* Geological Society, London, Memoirs, **20**, 17–59, https://doi.org/10.1144/GSL.MEM.2003.020.01.04

Walker, F., Schofield, N., Millett, J., Jolley, D., Hole, M. and Stewart, M. 2020. Paleogene volcanic rocks in the northern Faroe-Shetland Basin and Møre Marginal High: understanding lava field stratigraphy. *In:* Chiarella, D., Archer, S.G., Howell, J.A., Jackson, C.A.-L., Kombrink, H. and Patruno, S. (eds) *Cross-Border Themes in Petroleum Geology II: Atlantic Margin and Barents Sea.* Geological Society of London Special Publication, **495**. First published online 19 March 2020, https://doi.org/10.1144/SP495-2019-13.

Watton, T.J., Cannon, S., Brown, R.J., Jerram, D.A. and Waichel, B.A. 2014. Using formation micro-imaging, wireline logs and onshore analogues to distinguish volcanic lithofacies in boreholes: examples from Palaeogene successions in the Faroe-Shetland Basin, NE Atlantic. *In:* Cannon, S.J.C and Ellis, D. (eds) *Hydrocarbon Exploration to Exploitation West of Shetlands.* Geological Society of London Special Publication, **397**, 173–192, https://doi.org/10.1144/SP397.7

Watson, D., Schofield, N., Jolley, D., Archer, S., Finlay, A.J., Mark, N., Hardman, J. and Watton, T. 2017. Stratigraphic overview of Palaeogene tuffs in the Faroe-Shetland Basin, NE Atlantic Margin. *Journal of the Geological Society,* **174**, 627–645, https://doi.org/10.1144/jgs2016-132

Watson, D., Schofield, N., Maguire, A., Telford, C., Mark, N., Archer, S. and Hardman, J. 2019. Raiders of the Lost Mud: the geology behind drilling incidents within the Balder Formation around the Corona Ridge, West of Shetland. *Petroleum Geoscience,* 26(1), 110–125, https://doi.org/10.1144/petgeo2018-060

White, R.S., Spitzer, R., Christie, P.A.F., Roberts, A., Lunnon, Z., Maresh, J. and iSIMM Working Group 2005. Seismic imaging through basalt flows on the Faroes Shelf. *In:* Ziska, H., Varming, T. and Blotch, D. (eds) *Faroe Islands Exploration Conference: Proceedings of the 1st Conference*. Faroese Society of Sciences and Humanities, Tórshavn, 11–31.

White, R.S., Smith, L.K., Roberts, A.W., Christie, P.A.F., Kusznir, N. and Team iSimm 2008. Lower-crustal intrusion on the north Atlantic continental margin. Nature, **452**, 460–464, https://doi.org/10.1038/nature06687

Wrona, T., Magee, C., Fossen, H., Gawthorpe. R.L., Bell, R.E., Jackson, C.A.-L. and Faleide, J.I. 2019. 3-D seismic images of an extensive igneous sill in the lower crust. *Geology,* **47(8)**, 729–733, https://doi.org/10.1130/G46150.1

Ziska, H. and Anderson, C. 2005. Exploration Opportunities in the Faroe Islands. *In:* Ziska, H., Varming, T. and Blotch, D. (eds) *Faroe Islands Exploration Conference: Proceedings of the 1st Conference*. Faroese Society of Sciences and Humanities, Tórshavn, 146–162.

Ziska, H. and Varming, T. 2008. Palaeogene evolution of the Ymir and Wyville Thomson ridges, European North Atlantic margin. *In:* Johnson, H., Doré, A.G., Gatliff, R.W., Holdsworth, R., Lundin, E.R. and Ritchie, J.D. (eds) *The Nature and Origin of Compression in Passive Margins.* Geological Society of London Special Publication, **447**, 357–374, https://doi.org/10.1144/SP447.7

Tables

Table 1: *Key acquisition parameters of phase 1 and 2 of the 3D seismic survey used in this study.*

Acquisition Parameters	**Phase 1: Galloway 2013**	**Phase 2: Corona 2015**
Dual source depth (m)	9	9
Number of streamers	12	10
Streamer towing depth (m)	20	20
Streamer spacing (m)	100	100
Streamer cable length (m)	6000	7050
Near trace offset (m)	200	99
Shot interval (m)	25	25

Table 2: *Descriptions of the Colsay Member (T40-T45) units 1 to 4 within the Rosebank Field (Hardman et al. 2018; Duncan et al. 2020) and 213/23-1 (Eriboll) (213/23-1 Composite Well Log 1998; 213/23-1 Sedimentology & Petrography 1999). Porosities given for Colsay units 1 and 3 within 213/23-1 are based on petrography of Colsay 1 core (Fig. 10) (213/23-1 Sedimentology & Petrography 1999) and Colsay 3 cuttings (213/23-1 Final Geological Well Report 1999). Porosities given for Colsay units 1 and 3 within the Rosebank Field are average porosity ranges from Duncan et al. (2020). Visible porosities for Colsay 2 within the Rosebank Field are based on Rosebank exploration and appraisal wells 213/26-1 and 213/27-3Z.*

Colsay Unit	Rosebank Field	213/23-1 (Eriboll)
1	Siliciclastic successions of interbedded sandstones, siltstones and claystones with occasional volcaniclastic claystones and sandstones. Average gross thickness across the field is *c.* 56 m. Reservoir sandstones are described as very fine to medium grained (rarely coarse), sub-rounded to sub-angular, poorly cemented, and moderately to well sorted with average porosities of 21- 23%. Interpreted as braided fluvial sandstones within the T40 Colsay 1 interval and fully marine within the T45 Colsay 1 interval.	Siliciclastic and volcaniclastic sandstones, siltstones and claystones. Sandstones are very fine to medium grained, angular to sub-rounded, poor to well-sorted, grain supported, friable, with occasional calcareous cement. Highest point-counted porosities seen are 15% with others as low as 5%. Reservoir quality is considered poor, reflecting high proportions of clay matrix, calcite cement and grain compaction. 10 m of T45 Colsay 1 core (Fig. 10) contains flat to low-angle lamination, wave ripple lamination with local hummocky cross-stratification, bivalves, burrows, and plant fragments interpreted as shallow marine shelf deposits.
2	Thin siltstones, lignitic material and occasional volcaniclastic lithologies (siltstones and sandstones). Sandstones are described as fine (rarely coarse), well-sorted and angular with visible porosities described as poor to moderate.	Sandstones, claystones and volcaniclastic claystone. Sandstones are very fine to medium (locally coarse), sub-rounded to rounded, moderately sorted and friable with intermediate porosities.
3	Successions of sandstones, claystones and siltstones with influxes of volcaniclastic sandstone indicative of an estuarine environment, overlain by fluvial sediments sourced from the SW. Average gross thickness across the field is *c.* 28 m. Reservoir sandstones are very fine to fine grained, occasionally coarse, sub-angular to angular, well-sorted and poorly cemented with average porosities between 21-23%.	Sandstones, siltstones, claystones and volcaniclastic rocks (siltstone and claystone). Sandstones are very fine to fine, sub-angular to sub-rounded, moderately to poorly-sorted, friable, very micaceous and grain supported with no visible matrix or cement present and poor porosity. One residual oil show was observed within volcaniclastic siltstone at c. 2955 m MD (Fig. 10). Porosities of sandstone cuttings are described as intermediate to poor; no values are given.

4	Interbedded clastic and volcaniclastic claystones and siltstones, interpreted as pro-delta deposits. Average gross thickness of *c.* 22.5 m across the field. Sandstones are described as very fine, sub-angular to angular, well-sorted and thin.	Sandstones, claystones and volcaniclastic lithologies (sandstone, siltstone, and claystone). Sandstones are very fine to fine grained, sub-angular, moderately-sorted, grain supported, with occasional calcareous cement and oil shows. Oil show observed (3079 m MD) within a 25 m thick, friable, very fine to fine, sub-angular, moderately sorted reworked sandstone with 'loose' quartz grains.

Table 3: *Average petrophysical properties of the Carboniferous and Devonian intervals within 213/23-1 (Eriboll) and 213/25c-1V (North Uist) obtained from end of well reports (213/23-1 Final Geological Well Report 1999; 213/25c-1V End of Well Report 2013).*

213/23-1	**Carboniferous** (*c.* 3585-4028 m MD)	**Devonian** (4028 m MD - TD)
Porosity (%)	15	13
Net-to-gross (NTG)	0.52	0.22
Water Saturation (%)	68	77
213/25c-1V	**Carboniferous Upper Reservoir** (3974-4069 m MD)	**Devonian–Carboniferous Lower Reservoir** (4069-4773 m MD)
Gross thickness (m)	94.5	704
Net pay (m)	32.2	566*
Porosity (%)	14	11
Net-to-gross (NTG)	0.34	0.80
Water saturation (%)	56	82

**BP interpret no net pay due to high water saturations and lack of successful pressure tests (213/25c-1V End of Well Report 2013).*

Figure Captions

Fig. 1. (**a**) Map of the Faroe-Shetland Basin highlighting the main structural elements and study area. Note the presence of Cambo, Rosebank, and Clair Fields and other discoveries along the Corona and Rona intra-basinal highs (light grey). Map also shows coverage outline of the Corona 3D seismic survey and location of seismic lines shown in this study. (**b**) Map (a) overlain with key wells and fields discussed with pipeline infrastructure within the Faroe-Shetland Basin. Figure adapted from Ritchie *et al.* (2011) and Mark *et al.* (2018b) with structural lineaments (also referred to as transfer zones) and intra-basinal highs modified from Ellis *et al.* (2009) and Hardman *et al.* (2018).

Fig. 2. Faroe-Shetland Basin tectonic history and lithostratigraphy with various aspects of the basins petroleum system and associated discoveries. Numerical ages and chronostratigraphy are taken from the International Chronostratigraphic Chart 2020 (Cohen *et al.* 2013). Figure and lithostratigraphy is modified from Scotchman *et al.* (2006) and stratigraphic units (groups) from Ritchie *et al.* (2011). Plate tectonic events and UK Atlantic margin events are based on Scotchman *et al.* (2006), Ritchie *et al.* (2011) and Schöpfer & Hinsch (2019). Sea level curve is modified from Haq *et al.* (1987). Potential and proven source rocks are from both Scotchman *et al.* (2006) and Quinn *et al.* (2011). Play types are modified from numerous authors individually cited (Goodchild *et al.* 1999; Herries *et al.* 1999; Duncan *et al.* 2009; Larsen *et al.* 2010; Trice 2014; Ogilvie *et al.* 2015; Watson *et al.* 2019). Note: Wells and discoveries located along the Corona Ridge are shown with an asterisk (*) and Eriboll (213/23-1) contained only oil shows and is added for context.

Fig. 3. NW-SE regional seismic line and geoseismic interpretation from North Uist (213/25c-1V) on the Corona Ridge, through South Uist (214/21a-2) and onto the West Shetland High. Seismic data from the North Sea Transition Authority National Data Repository was acquired by PGS for Total E&P U.K. Ltd (Corona & Galloway 3D, Flett Phase 1 & 2 3D) and by WesternGeco (SE Clair 2014 3D) for BP and partners. The PGS FSB MegaSurvey Plus is shown courtesy of PGS who granted permission to publish the line. Location of the seismic line transect is shown in Fig. 1a.

Fig. 4. Paleogene stratigraphy of the Faroe-Shetland Basin, with British Geological Survey (Ritchie *et al.* 2011) and BP T-sequence framework (after Ebdon *et al.* 1995) modified from Schofield & Jolley (2013) and Jolley *et al.* (2021). Local assemblage zone, LAZ (1), defined by Schofield & Jolley (2013) and updated by Jolley *et al.* (2021).

Fig. 5. NE-SW 3D Corona seismic line and geoseismic interpretation through the central-northern Corona Ridge and exploration wells 213/23-1 (Eriboll) and 213/23c-1V (North Uist). Seismic data was acquired by PGS for Total E&P U.K. Ltd and is from the North Sea Transition Authority National Data Repository. Location of the seismic line transect is shown in Fig. 1a. Note: (1) Faults shown in red correspond to oblique N-S & NNW-SSE-trending faults at Top Crystalline Basement (Fig. 14) and (2) the box on seismic section (top left) highlights the presence of a similar Flett Formation seismic response to that of the Rosebank Field (Hardman *et al.* 2018, p. 77, Fig. 7a; Poppitt *et al.* 2018, p. 378, Fig. 6; Duncan *et al.* 2020, p. 985, Fig. 6).

Fig. 6. NW-SE 3D Corona seismic line and geoseismic interpretation through the central-northern Corona Ridge, well 213/23-1 (Eriboll) and the Flett sub-basin. Seismic data was acquired by PGS for

Total E&P U.K. Ltd and is from the North Sea Transition Authority National Data Repository. Location of the seismic line transect is shown in Fig. 1a.

Fig. 7. NW-SE 3D Corona seismic line and geoseismic interpretation through well 213/25c-1V (North Uist) on the central-northern Corona Ridge and well 214/21a-2 (South Uist) drilled just off the central-northern Corona Ridge within the Flett sub-basin. Seismic data was acquired by PGS for Total E&P U.K. Ltd and is from the North Sea Transition Authority National Data Repository. Location of the seismic line transect is shown in Fig. 1a.

Fig. 8. NW-SE seismic line and geoseismic interpretation through the central-northern Corona Ridge within the NW end of the dataset. Note the unusual Cretaceous seismic response (usually opaque mudstones), possibly reflecting sand-claystone intervals or limestone 'stringers'. Seismic data was acquired by PGS for Total E&P U.K. Ltd and is from the North Sea Transition Authority National Data Repository. Location of the seismic line transect is shown in Fig. 1a.

Fig. 9. Pre-drill (prognosed) and post-drill (actual) lithologies (with gramma ray) and lithostratigraphy of wells (**a**) 213/23-1 (Eriboll), (**b**) 213/23c-1V (North Uist) and (**c**) 214/21a-2 (South Uist) with relevant well data obtained, and hydrocarbon shows encountered. Note the inconsistencies in well tops, e.g., the Top Paleocene varying between the Top Balder Fm (213/23-1), the Top Flett Fm (213/25c-1V) and the Top Lamba Fm (214/21a-2). Prognosed (pre-drill) and actual (post-drill) lithostratigraphy and well tops are unmodified from those given within composite logs and end of well reports (213/23-1 Final Geological Well Report 1999; 214/21a-2 End of Well Report 2010; 213/25c-1V End of Well Report 2013). Abbreviations; CKG, Cromer Knoll Group; EOWR, End of Well Report; ORS, Old Red Sandstone; UCG, Upper Clair Group; ?, Undifferentiated.

Fig. 10. Original composite log lithologies (also see Fig. 9a) and reinterpreted lithologies of the Colsay Member (sequence T40-T45) within well 213/23-1 (Eriboll) with relevant intervals of resistivity image logs used to reinterpret the section. Note: (1) Colsay units 1 to 4 were assigned based on biostratigraphy suggestive of different depositional environments generally associated with each unit, (2) where core plug lithology is not consistent with composite log lithology, lithology is listed in bold, (3) the different depth scales of resistivity image logs and (4) for location of Fig. 10f, see Fig. 10c.

Fig. 11. Lithostratigraphic and sequence correlation of the T40-T45 Colsay Member (Colsay 1 to 4 units) from Rosebank appraisal well 213/27-2 through Rosebank exploration well 213/27-3Z and along the central-northern Corona Ridge into 213/23-1 (Eriboll). The main reservoirs within the Rosebank Field area are within the Colsay 1 and Colsay 3 intervals (Duncan *et al.* 2020). Note: The Upper Thanetian Unconformity (UTU) marks the top of sequence T38 (see Fig. 4 and Jolley *et al.* 2021).

Fig. 12. (**a**) Resistivity image logs through the proposed 'Triassic?' (reinterpreted by this study as middle Carboniferous) and middle Carboniferous sections from 3689-3831 m MD within 213/23-1, with bedding sinusoids, resistive and conductive fractures, and their corresponding tadpole plot. Note: A structural dip of 55° has not been removed and locations of core 4 have been depth shifted based on a -1.2 m core to wireline shift (213/23-1 FMI Structural & Sedimentological Interpretation 1999). (**b**) Rose diagram showing the strike of resistive and conducive fractures interpreted within the section shown in (a). (**c**) Various photos of core 4 obtained within the middle Carboniferous

(previously interpreted post-drill as 'Triassic?'), locations of where core 4 was recovered are shown within (a). (**d**) Various photos of core 5 obtained within the middle Carboniferous interval with key descriptions and an example of core petrography (213/23-1 Sedimentology & Petrography 1999) showing hydrocarbons present within pores. Note: No image logs were obtained over the core 5 interval which was obtained from a deeper middle Carboniferous section. Core photos from BGS (2021).

Fig. 13. Original post-drill stratigraphy (left, also see Fig. 9a, taken directly from 213/23-1 Final Geological Well Report 1999) and reinterpreted (revised by this study) stratigraphy and lithology (reinterpreted for Colsay Member) of well 213/23-1, with gamma ray (GR) and neutron-density wireline logs, and relevant location of figures contributing to the reinterpretation of well 213/23-1 (Figs 10, 11 & 12). Top Palaeocene pick is based on the palynofloral stratigraphy by Jolley *et al.* (2021). Middle to upper Eocene T-Sequence intervals taken from Stoker *et al.* (2012). Note (1) we interpret the Flett Formation to be 228 m thicker than interpreted post-drill (194 m), (2) our reinterpretation of the 'Triassic?' section as a continuation of the underlying middle Carboniferous strata, (3) the section assigned 'Devono/Carboniferous' post-drill is now assigned to the Devonian and (4) the Devonian-Carboniferous section has been split into the Lower and Upper Clair Group. Abbreviations; CKG, Cromer Knoll Group; ORS, Old Red Sandstone; ?, Undifferentiated.

Fig. 14. (**a**) Top Crystalline Basement surface time–structure map including structural elements mapped, note the presence of oblique faults (in red) trending N-S and NNW-SSE, see also Fig. 5 for seismic through oblique faults. (**b**) Top Crystalline Basement surface time–structure map and structural elements (a) with the area considered the central-northern Corona Ridge (transparent grey) by this study (as defined by Peacock & Banks 2020). Note (1) the series of lows (mini-basins) between the sections of crystalline basement within the NE of the dataset, (2) possible remnants of an intermontane basin labelled on the Corona Ridge and (3) the small map (Fig. 14b bottom right) showing the previous interpretation of the Corona Ridge taken from Fig. 1 (Ellis *et al.* 2009).

Fig. 15. Time surfaces with structural elements of the (**a**) base Cretaceous (oblique fault in red), (**b**) Top Cretaceous, (**c**) near Top Paleocene and (**d**) Top Flett Formation within the study area. Note (1) wells shown in red reflect where wells have penetrated the surface, (2) faults shown within the near Top Palaeocene (c) and Top Flett Formation (d) are all minor faults.

Fig. 16. Isochron time maps of the (**a**) Pre-Cretaceous (Devonian-Carboniferous and Jurassic) based on Basement (Fig. 14a) to base Cretaceous (Fig. 15a), with relevant structural elements (oblique fault shown in dark red). Due to the absent (e.g. 213/23-1) and thin (e.g. 213/25c-1V) presence of Jurassic encountered on the central-northern Corona Ridge along the structural high, the isochron can be used to infer Devonian-Carboniferous thicknesses. Note: We interpret no Triassic present in the study area. (**b**) Cretaceous, (**c**) Paleocene and (**d**) Flett Formation within the study area. Note (1) wells shown in red reflect where wells have penetrated the interval, and (2) where thicknesses of both the Paleocene (c) and Flett Formation (d) are less than 100 ms, intervals may be absent (e.g., Paleocene T10-T38 interval is absent in 213/23-1).

Fig. 17. Thickness maps of igneous intrusions emplaced within the Phanerozoic sedimentary sequences above the central-northern Corona Ridge showing (**a**) 1/4 wavelength thickness and (**b**) 1/8 wavelength thickness scenarios, both of which incorporate the ratio of 1:1.4-metre of imaged to unimaged igneous material (*see* Mark *et al.* 2018a). Figure highlights the much thicker pile of

intrusions within the Flett and Sissal sub-basins versus the lack of emplacement into Phanerozoic sedimentary sequences overlying the central-northern Corona Ridge (CR). Note (1) grey structural elements outside of the study area are based on Fig. 1 (Ellis *et al.* 2009) and (2) transparent grey area within the study area corresponds to the crystalline basement structure of the central-northern Corona Ridge (CR) interpreted by this study (see Fig 14b).

Figure 1

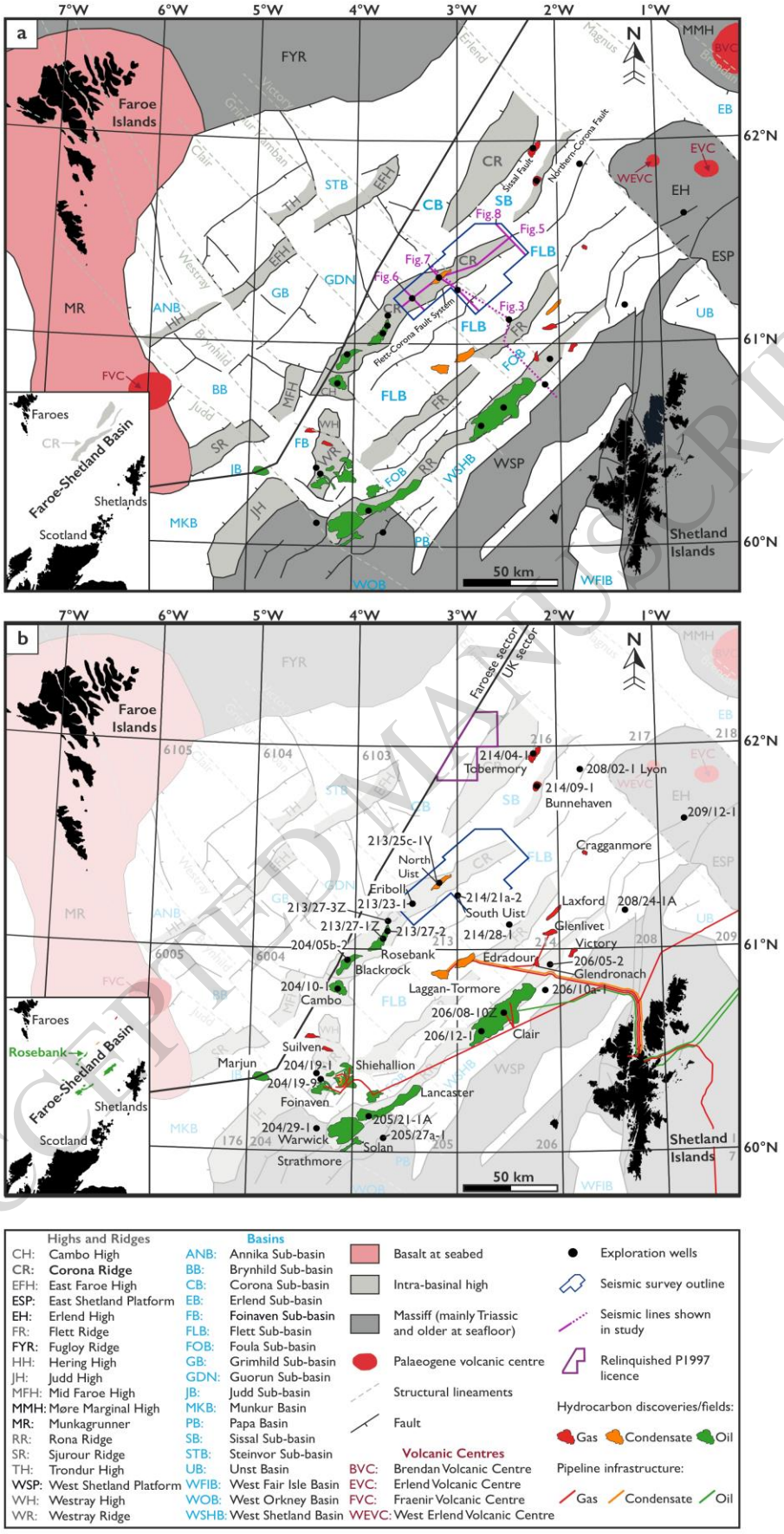

Figure 2

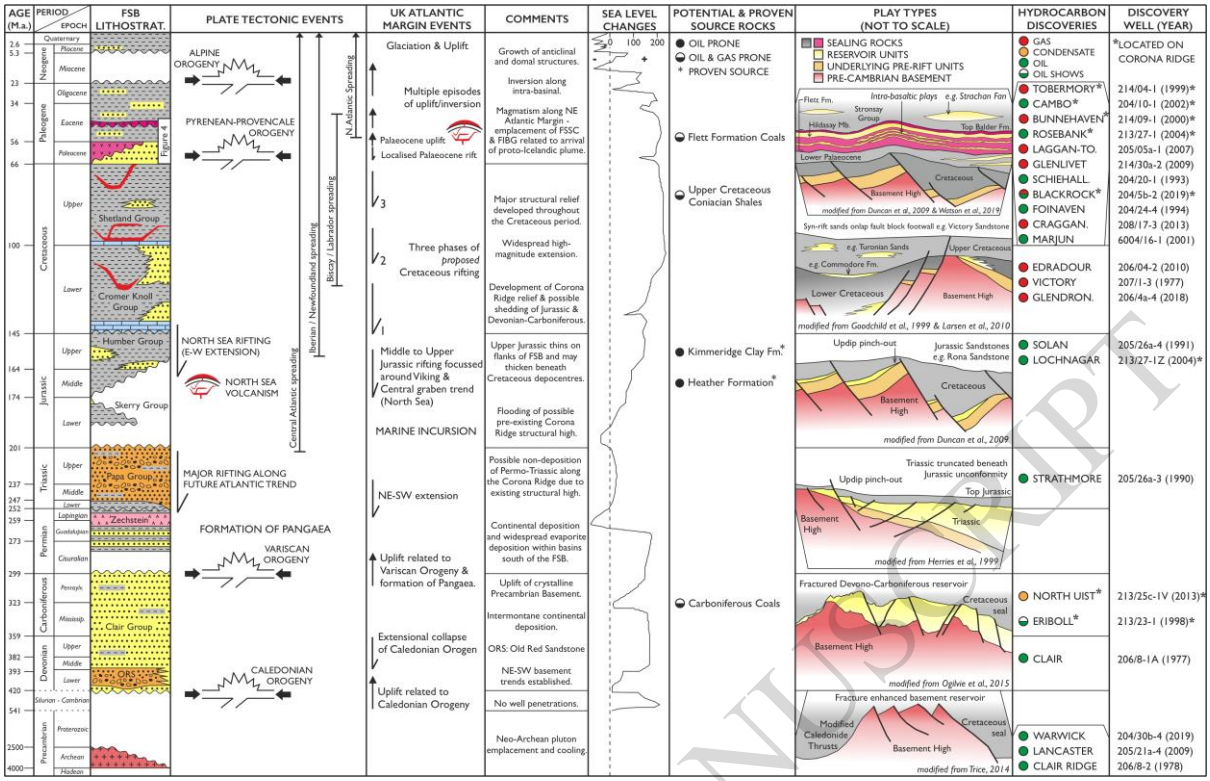

Figure 3

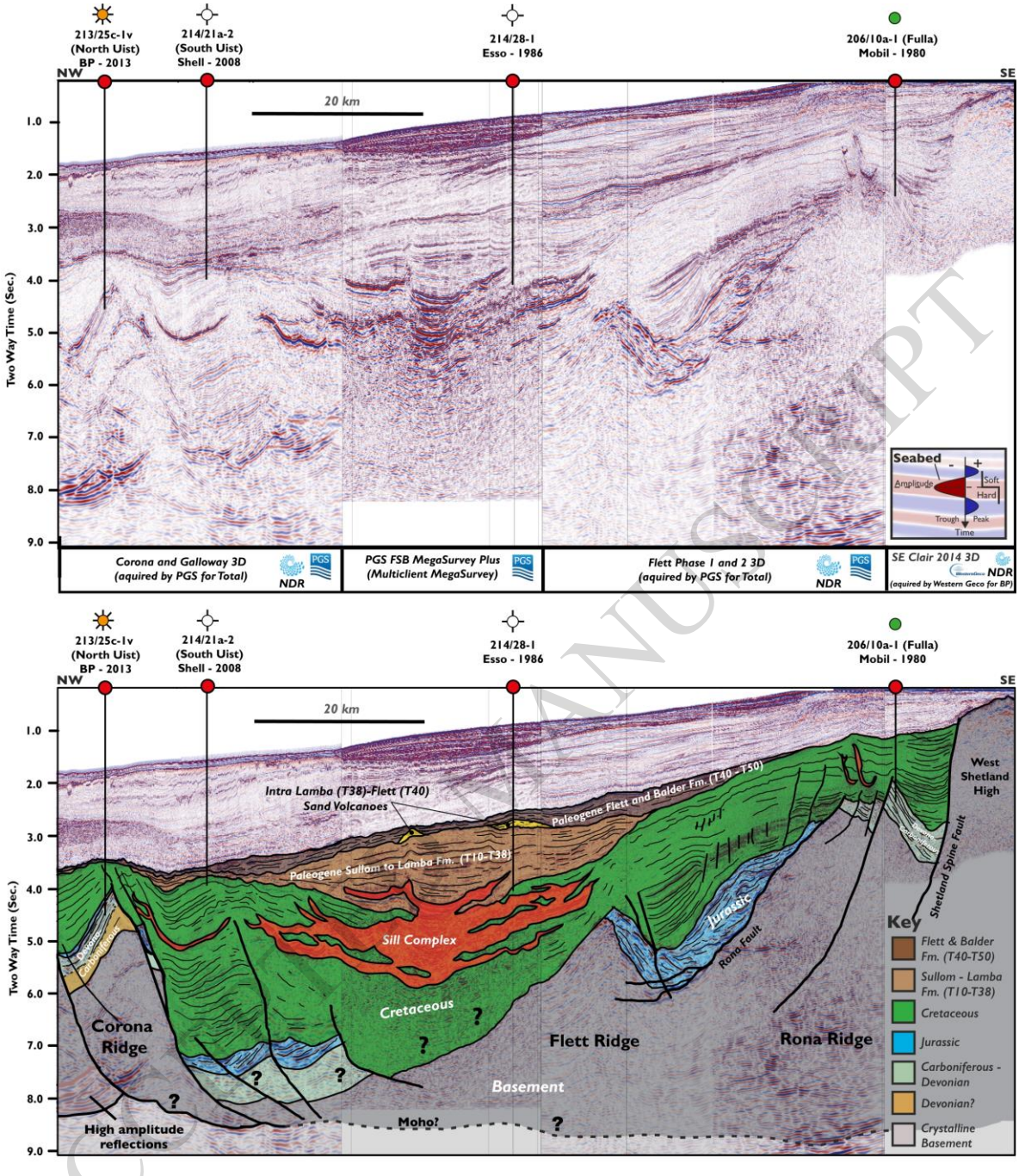

Figure 4

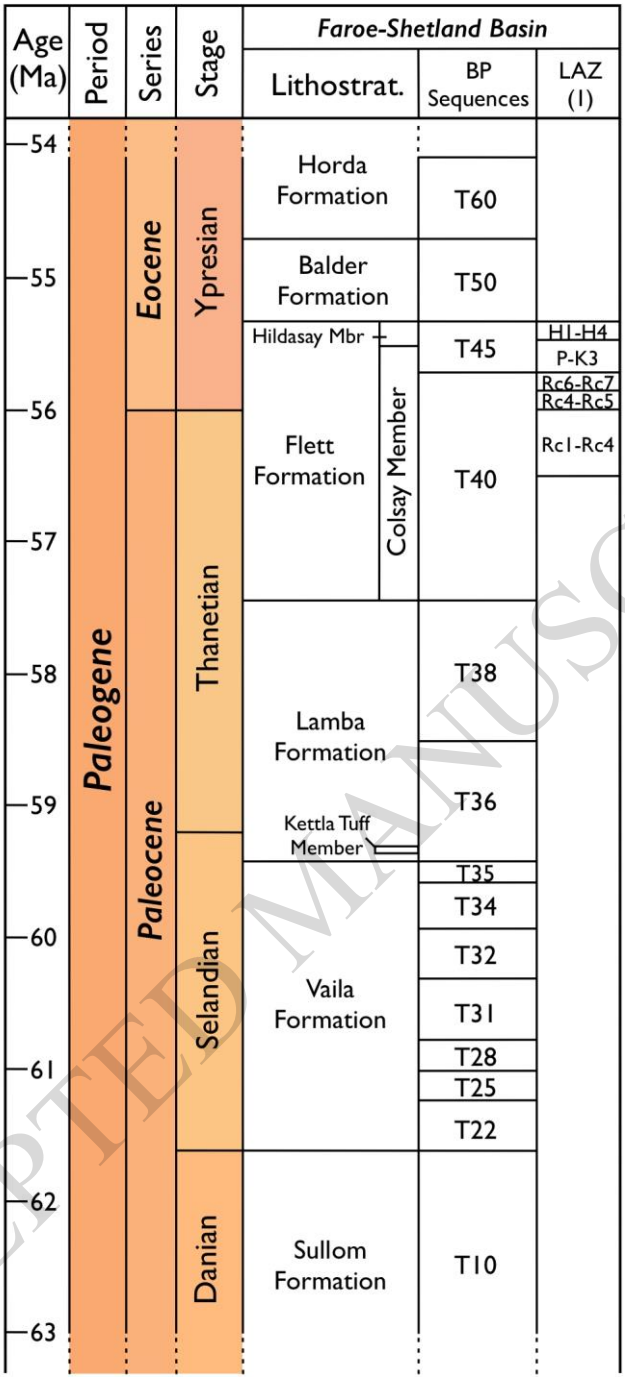

Figure 5

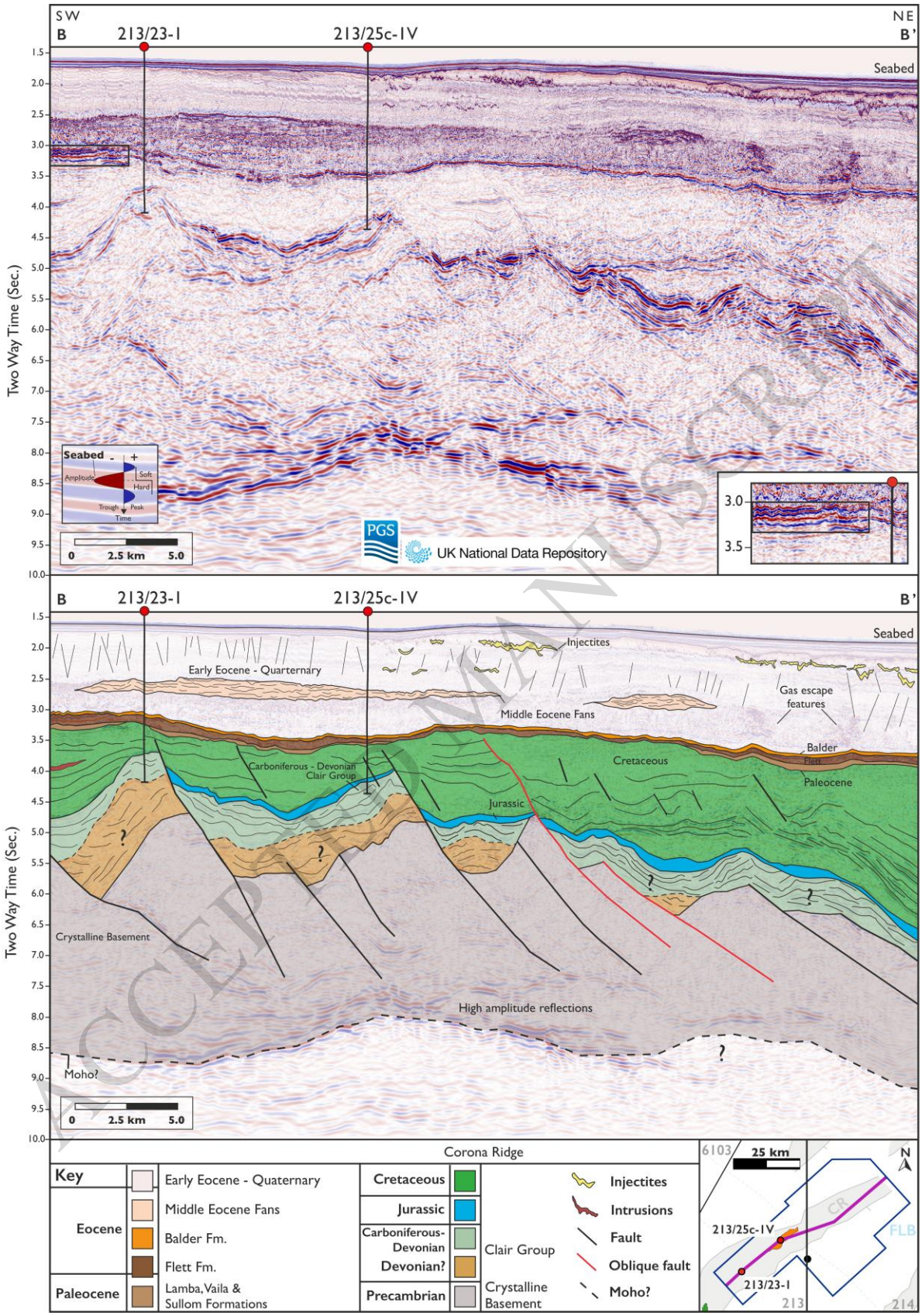

Figure 6

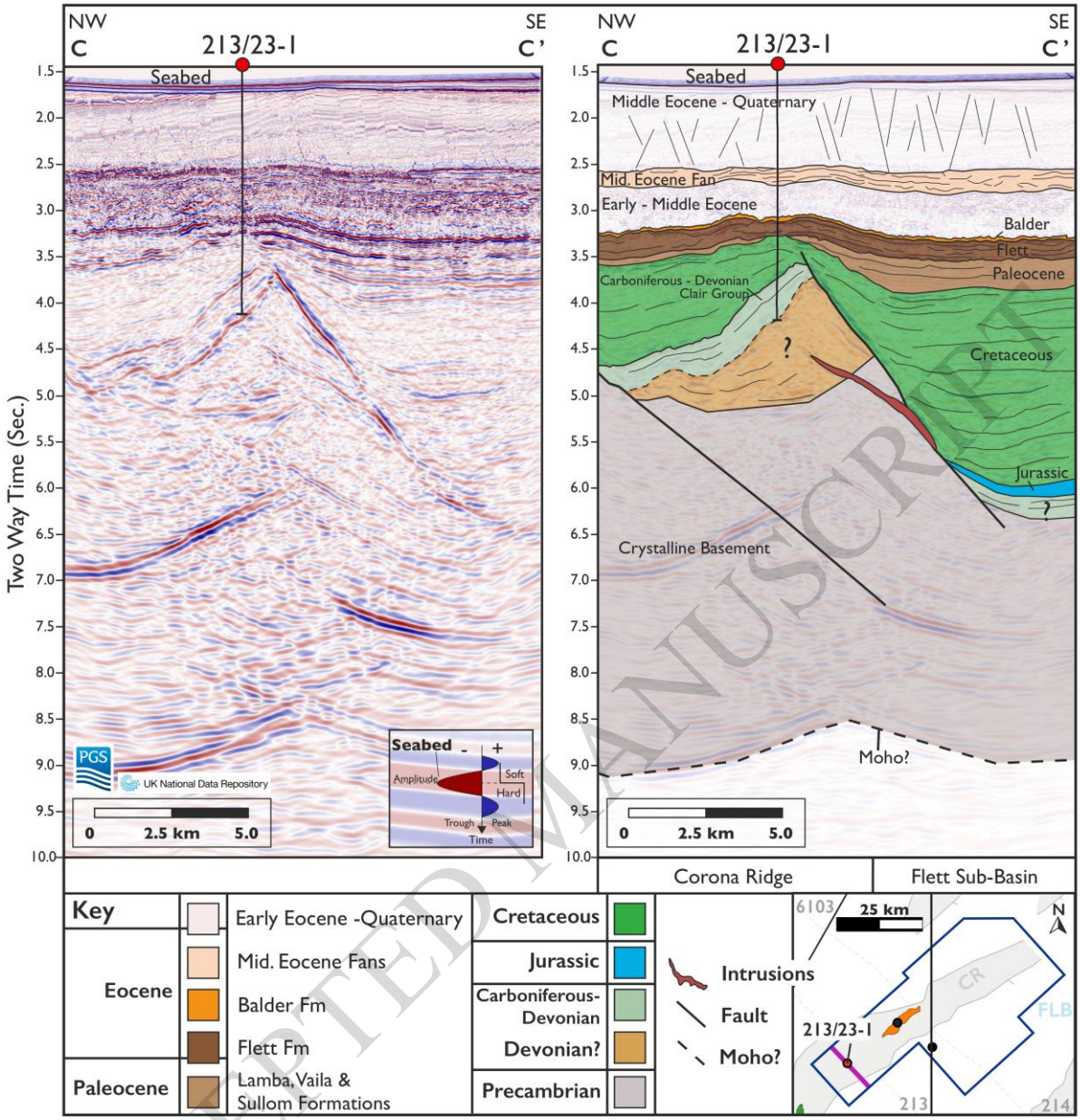

Figure 7

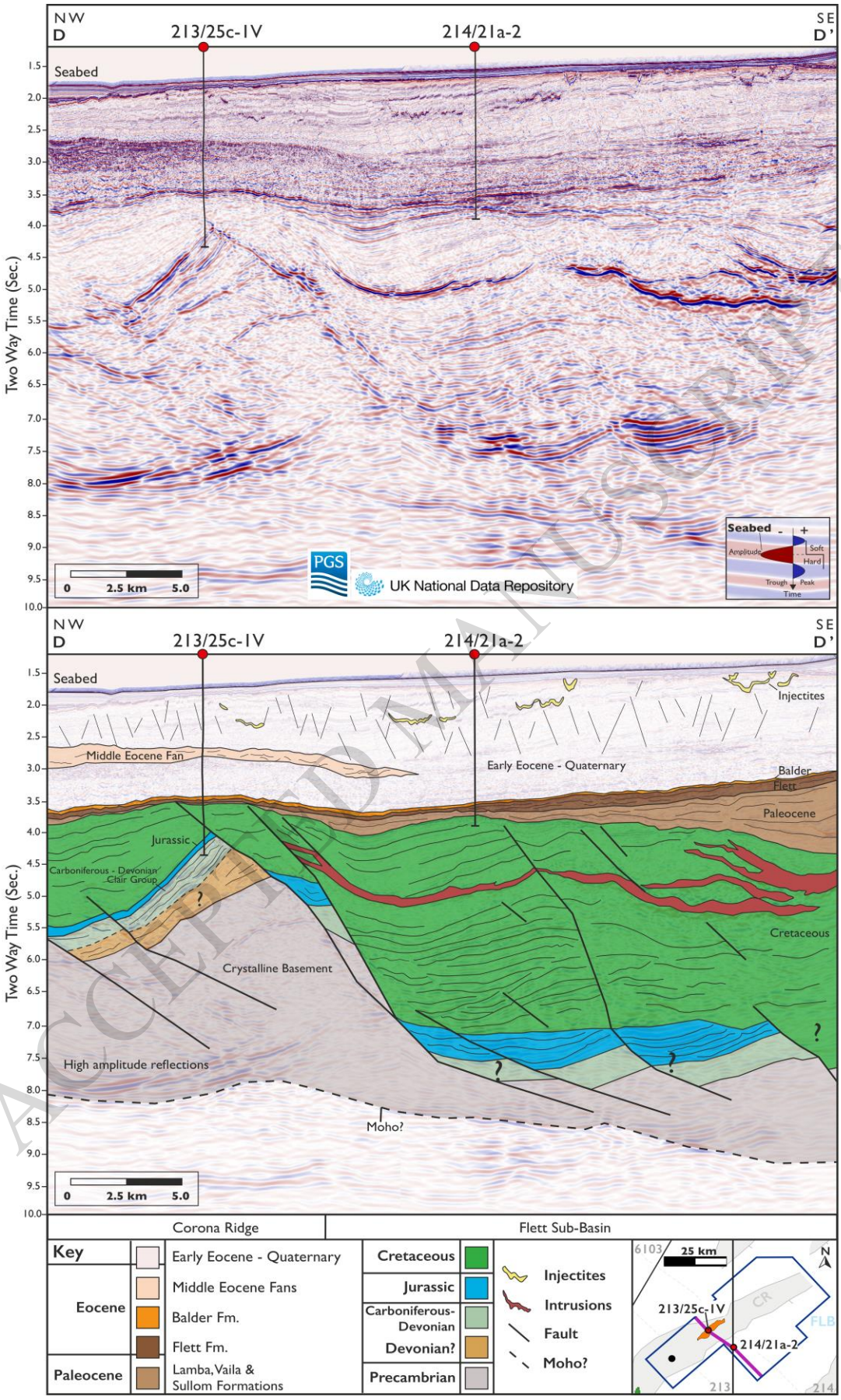

Figure 8

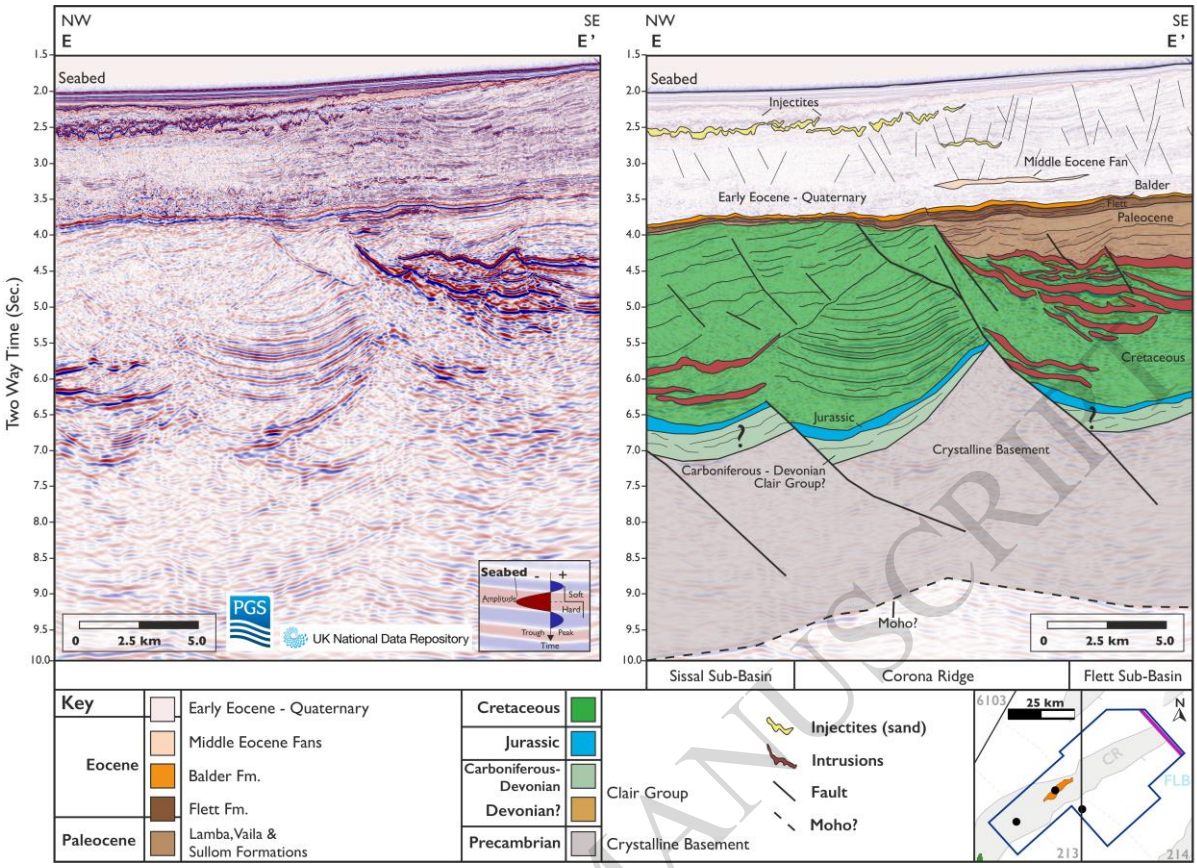

Figure 9

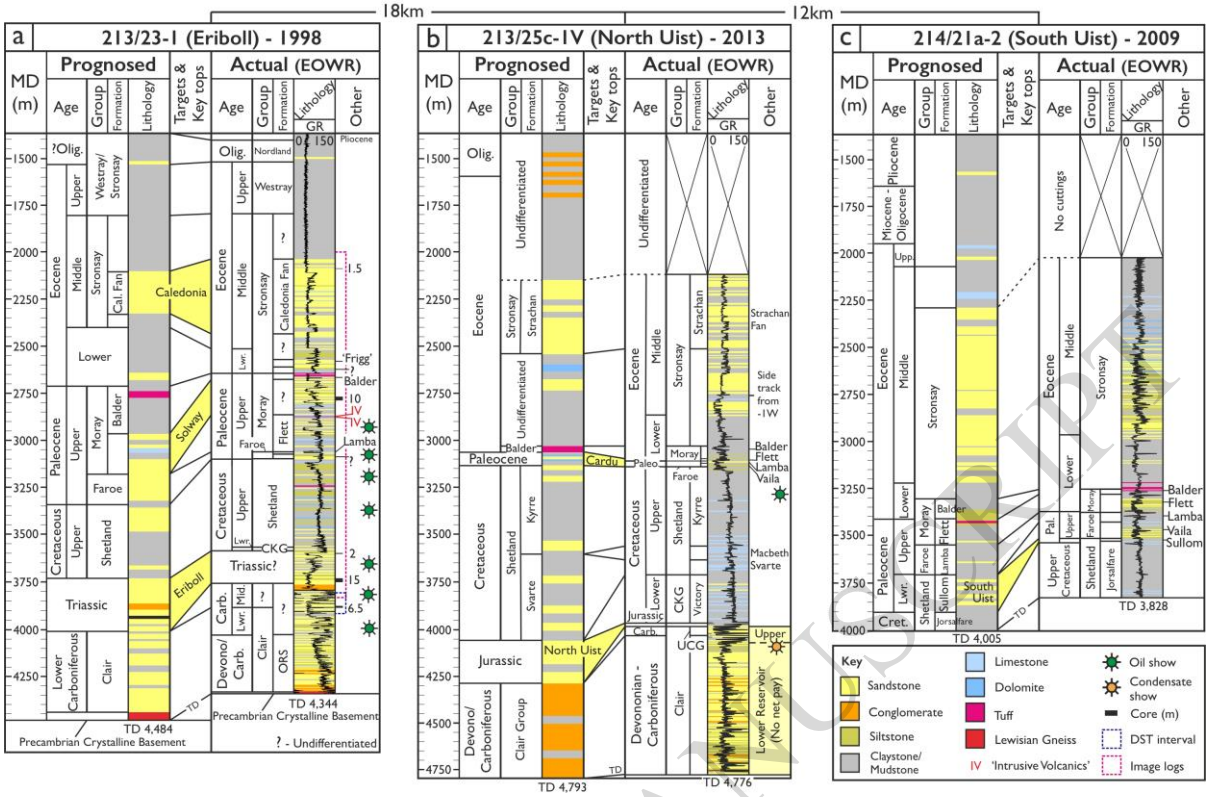

Figure 10

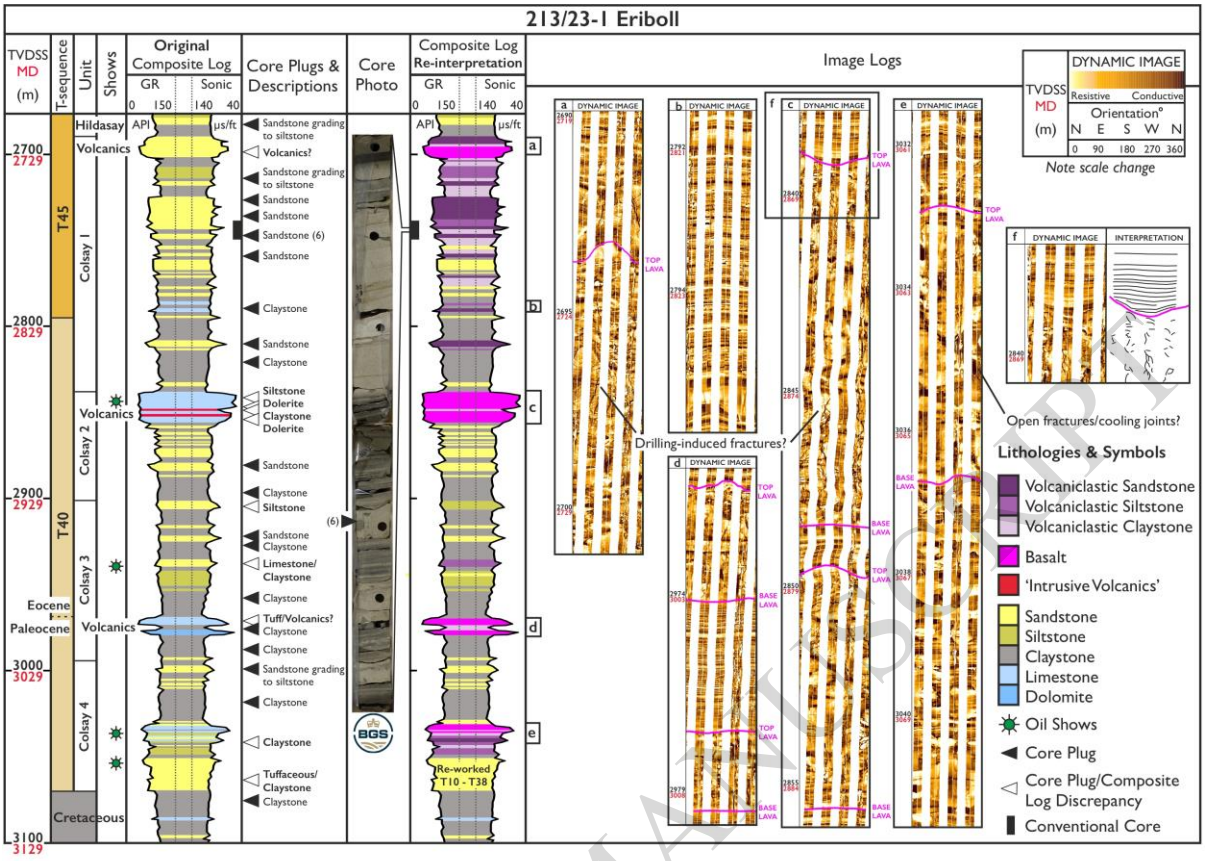

Figure 11

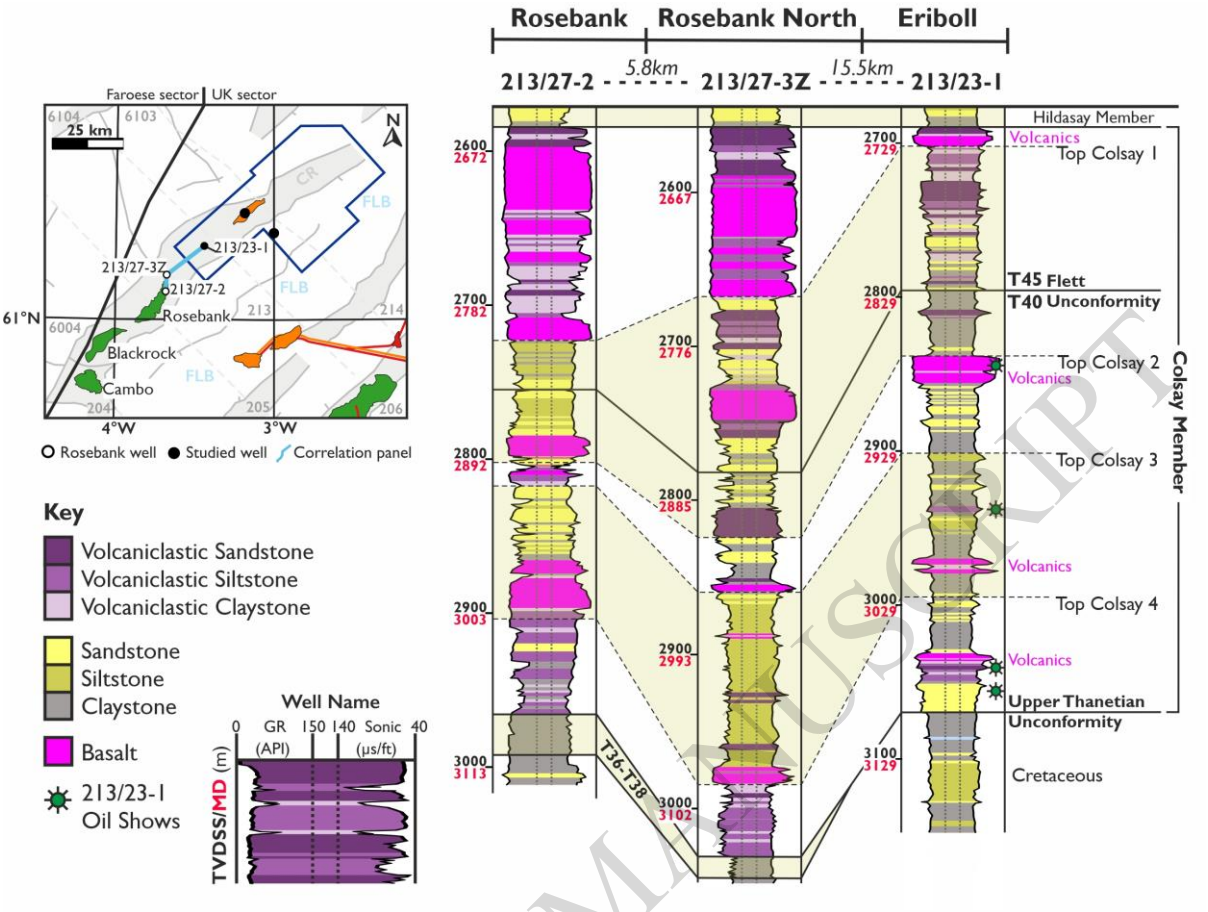

Figure 12

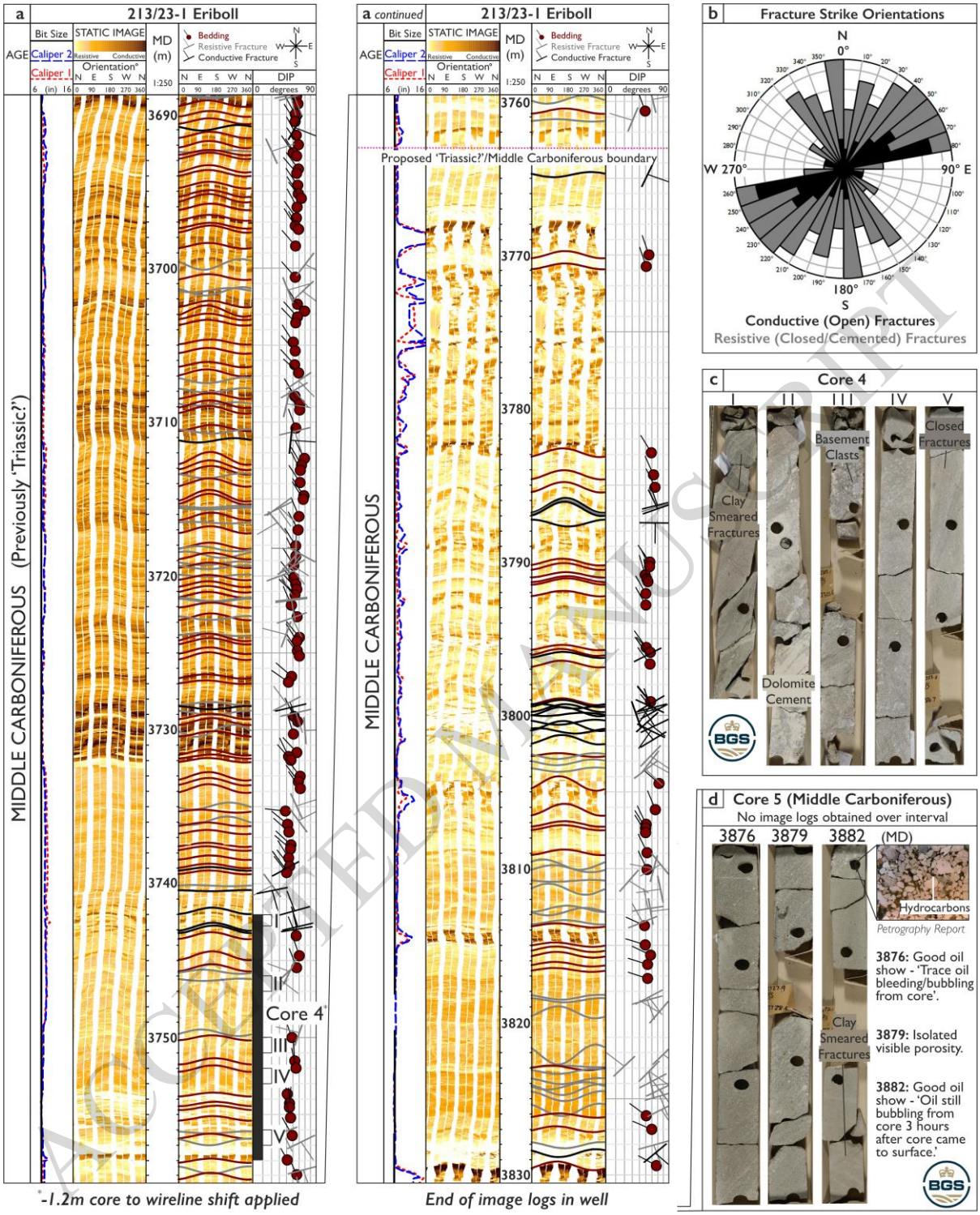

Figure 13

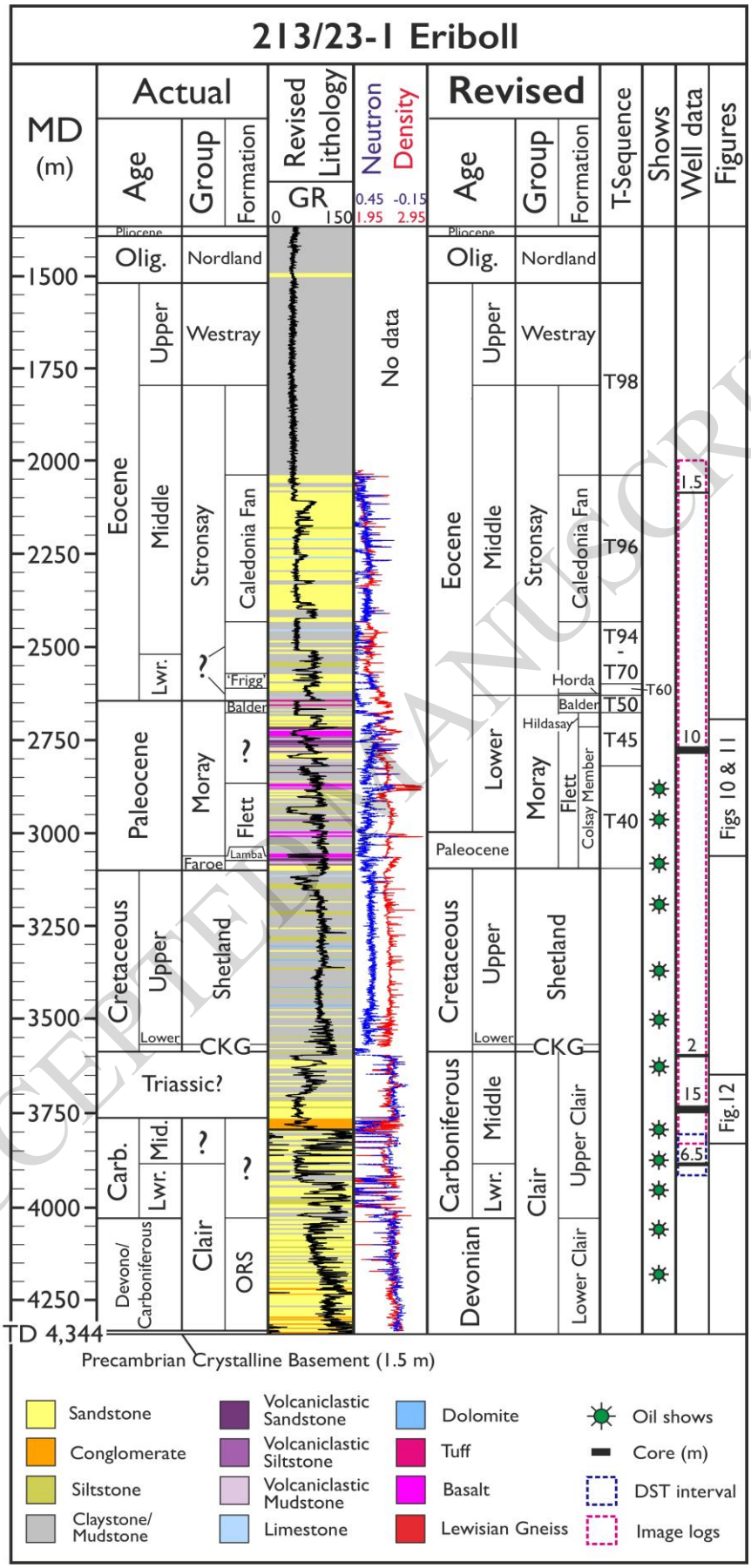

Figure 14

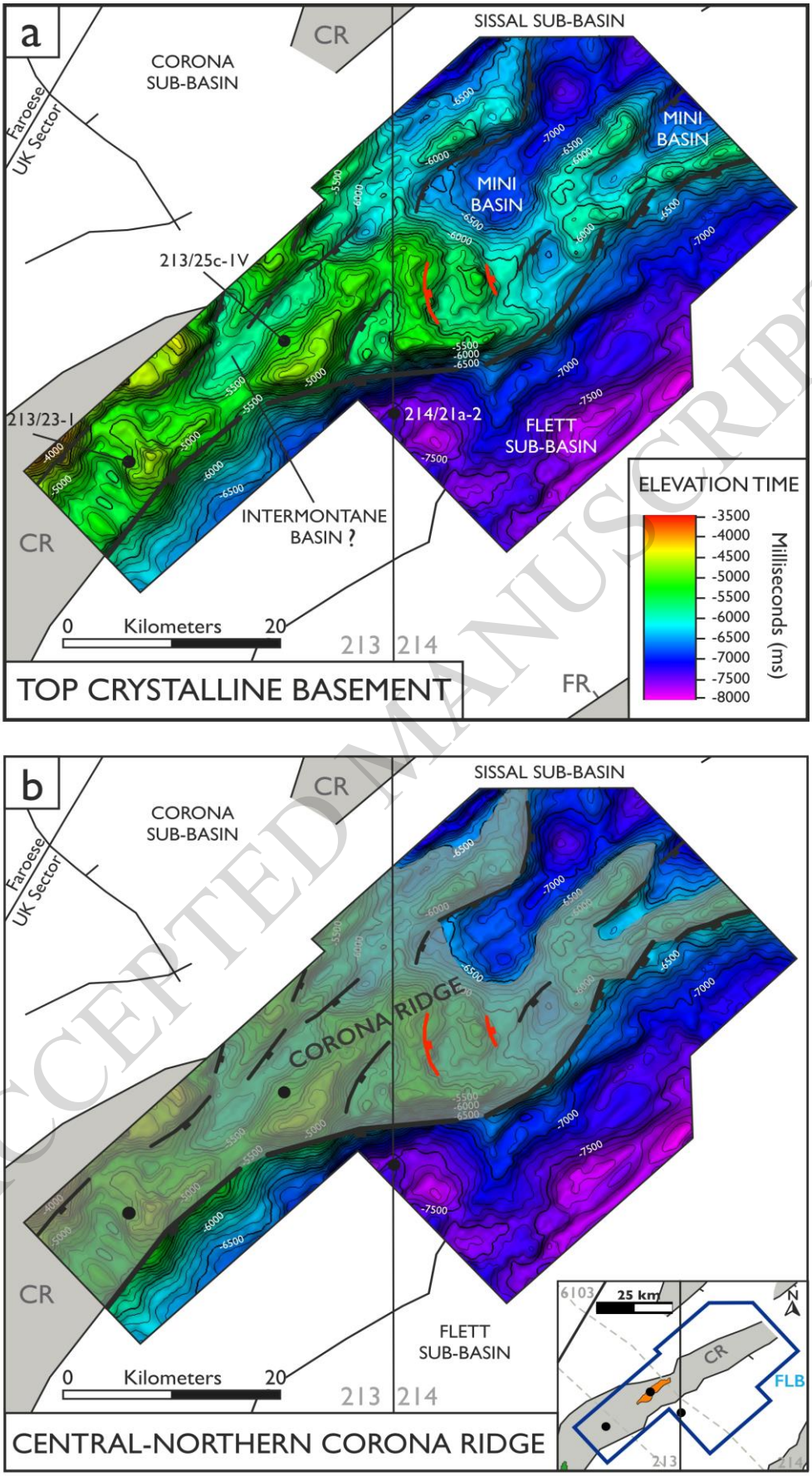

Figure 15

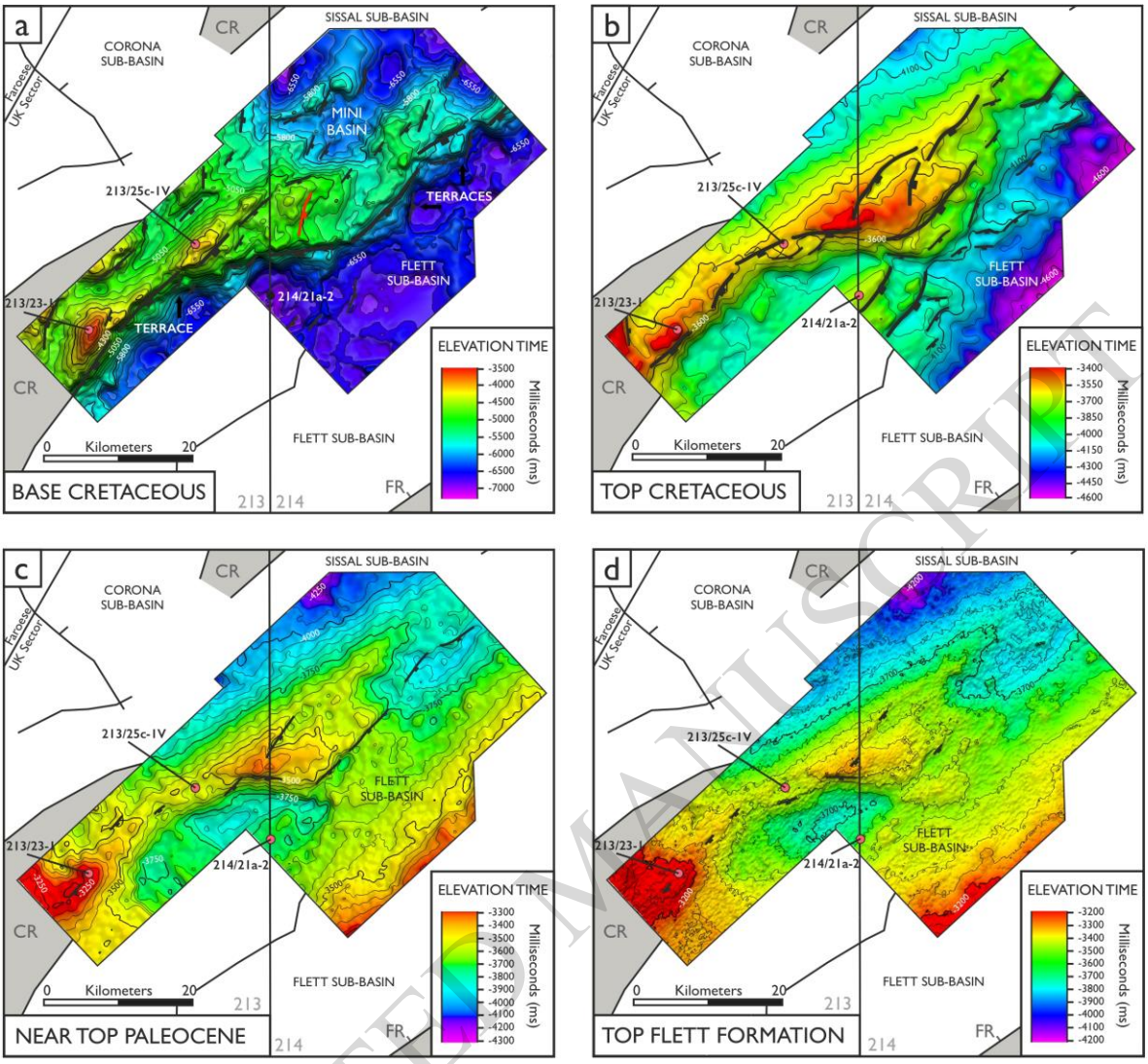

Figure 16

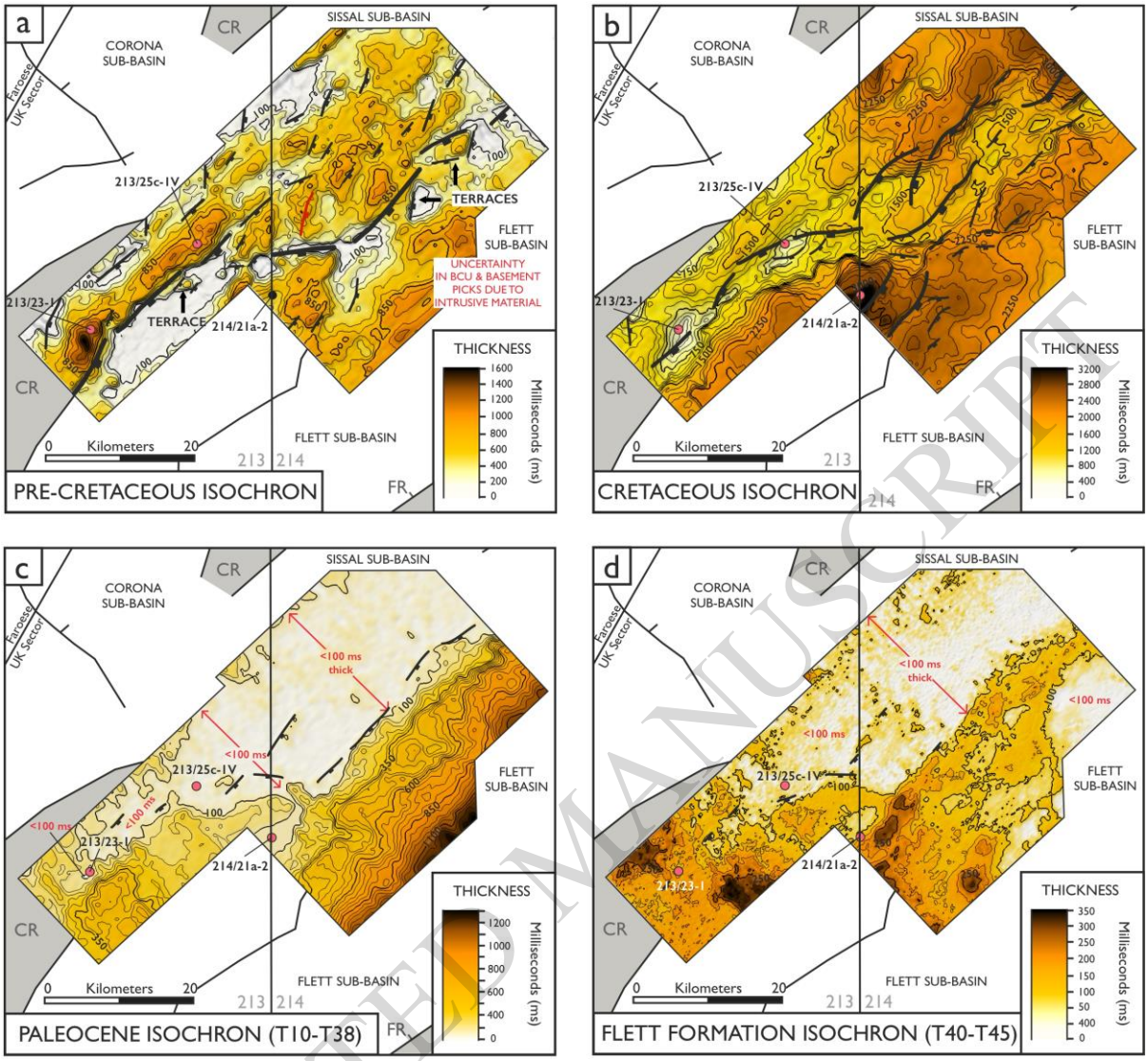

Figure 17